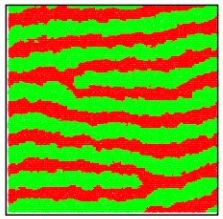

Mecánica Estadística y formación de patrones en películas magnéticas ultra-delgadas

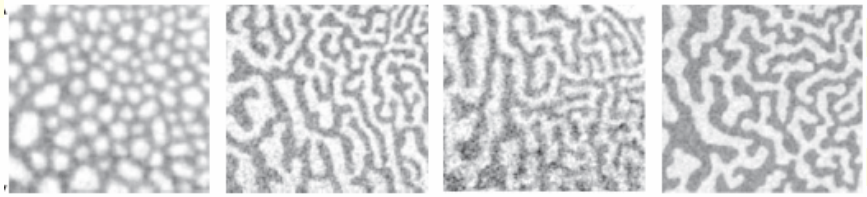

Facultad de Matemática, Astronomía y Física
Universidad Nacional de Córdoba

- Francisco A. Tamarit
- Orlando V. Billoni
- Pablo M. Gleiser (CAB)
- Hugo Toloza (UNL)
- Marianela Carubelli
- Santiago Pighin
- Ezequiel E. Ferrero

Universidade Federal do Rio Grande do Sul, Porto Alegre, Brasil

- Daniel A. Stariolo
- Mateus Fontana Michelon
- Lucas Nicolao

Laboratorio de Microestructras

Swiss Federal Institue of Technology Zurich, ETH, Suiza

- Danilo Pescia
- Alessandro Vindigni
- Oliver C. Portmann

Películas magnéticas ultra-delgadas

- Películas de Fe en Cu ó Fe/Ni/Cu
- Crecimiento epitaxial en ultra-alto vacío (~ 10^{-10} mbar)

- Películas ultra-delgadas: espesor $\Delta \leq$ 5 monocapas
- Fe: estructura fcc
- Interacciones de intercambio ferromagnéticas

Motivación

- Mecánica estadística: comportamiento crítico sumamente rico
- "Sistema modelo" para entender sistemas bidimensionales con interacciones competitivas mas complejos (ej., monocapas lipídicas, copolímeros de bloque, ferrofluidos, etc.).

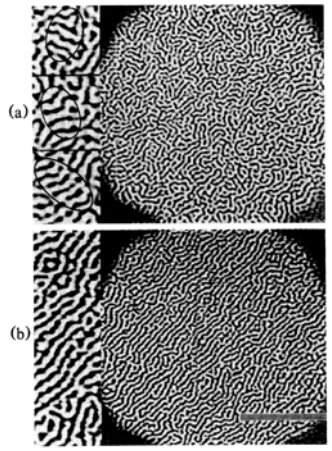

VOLUME 70, NUMBER 11 PHYSICAL REVIEW LETTERS 15 MARCH 1993

Isotropic and Aligned Stripe Phases in a Monomolecular Organic Film

M. Seul and V. S. Chen
AT&T Bell Laboratories, Murray Hill, New Jersey 07974
(Received 15 June 1992)

Interacciones microscópicas

INTERCAMBIO:

$$H_{ex} = -J_{ex} \sum_{<i,j>} \boldsymbol{\sigma}_i . \boldsymbol{\sigma}_j$$

$\boldsymbol{\sigma}_i$: spines clásicos

$|\boldsymbol{\sigma}_i| = 1$

<i,j>: suma sobre 1ros vecinos

ANISOTROPÍA MAGNETO CRISTALINA:

$$H_{an} = -\sum_i \left(\alpha_x \left(\sigma_i^x\right)^2 + \alpha_y \left(\sigma_i^y\right)^2 + \alpha_z \left(\sigma_i^z\right)^2 \right)$$

INTERACCIONES DIPOLARES

$$H_{dip} = J_{dip} \sum_{(i,j)} \left(\frac{\boldsymbol{\sigma}_i . \boldsymbol{\sigma}_j}{r_{ij}^3} - 3 \frac{(\boldsymbol{\sigma}_i . \mathbf{r}_{ij})(\boldsymbol{\sigma}_j . \mathbf{r}_{ij})}{r_{ij}^5} \right)$$

(i,j): suma todos los pares *i j*

$\mathbf{r}_{ij}$: distancia entre *i j*

~2 D:

ANISOTROPÍA MAGNETO CRISTALINA: → ANISOTROPÍA SUPERFICIAL

$$\alpha_z >> \alpha_x, \alpha_y$$

$$H_{an} = -\alpha_z \sum_i \left(\sigma_i^z\right)^2$$

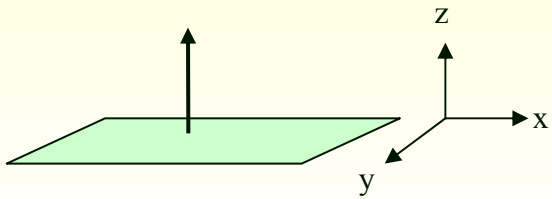

INTERACCIONES DIPOLARES $H_{dip} = J_{dip} \sum_{(i,j)} \left(\frac{\boldsymbol{\sigma}_i . \boldsymbol{\sigma}_j}{r_{ij}^3} - 3 \frac{(\boldsymbol{\sigma}_i . \mathbf{r}_{ij})(\boldsymbol{\sigma}_j . \mathbf{r}_{ij})}{r_{ij}^5} \right)$

Anisotropía de forma

$$H_f = -3\, J_{dip} \sum_{(i,j)} \left(\frac{(\boldsymbol{\sigma}_i . \mathbf{r}_{ij})(\boldsymbol{\sigma}_j . \mathbf{r}_{ij})}{r_{ij}^5} \right) \longrightarrow$$

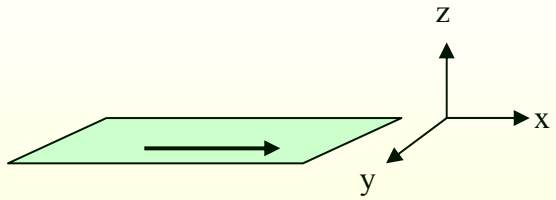

Ej., estado magnetizado uniformemente $\boldsymbol{\sigma}_i = \mathbf{m} \quad \forall i \quad H_f = -3\, J_{dip} \sum_{(i,j)} \frac{(\mathbf{m}.\mathbf{r}_{ij})^2}{r_{ij}^5}$

$$H = H_{ex} + H_{dip} + H_{an}$$

intercambio: $$H_{ex} = -\delta \sum_{<i,j>} \boldsymbol{\sigma}_i . \boldsymbol{\sigma}_j$$

dipolar: $$H_{dip} = \sum_{(i,j)} \left(\frac{\boldsymbol{\sigma}_i . \boldsymbol{\sigma}_j}{r_{ij}^3} - 3 \frac{(\boldsymbol{\sigma}_i . \mathbf{r}_{ij})(\boldsymbol{\sigma}_j . \mathbf{r}_{ij})}{r_{ij}^5} \right)$$

Anisotropía superficial $$H_{an} = -\eta \sum_i {}^{*} \left(\sigma_i^z \right)^2$$

$$\eta \equiv \frac{\alpha_z}{J_{dip}}$$

$$\delta \equiv \frac{J_{ex}}{J_{dip}}$$

Transición de reorientación

Teoría RG: predice una SRT a una temperatura T_R finita

VOLUME 65, NUMBER 20 PHYSICAL REVIEW LETTERS 12 NOVEMBER 1990

Perpendicular versus In-Plane Magnetization in a 2D Heisenberg Monolayer at Finite Temperatures

D. Pescia [1] and V. L. Pokrovsky [2],[a]

[1] *2. Physikalisches Institut der Rheinisch-Westfälische Technische Hochschule Aachen, D-5100 Aachen, Federal Republic of Germany*

[2] *Institut für Festkörperforschung des Forschungszentrums Jülich, D-5170 Jülich, Federal Republic of Germany*

(Received 16 July 1990)

VOLUME 64, NUMBER 26 PHYSICAL REVIEW LETTERS 25 JUNE 1990

Reversible Transition between Perpendicular and In-Plane Magnetization in Ultrathin Films

D. P. Pappas, K.-P. Kämper, and H. Hopster
Department of Physics and Institute for Surface and Interface Science, University of California, Irvine, California 92717
(Received 11 April 1990)

- Muestras crecidas a 100 K y recocidas a temperatura ambiente de Fe en Cu(100)
- Magnetización remanente paralela y perpendicular a la película mediante análisis de polarización de electrones secundarios
- Transición de reorientación sin transformación estructural para $\Delta \leq 5$ ML

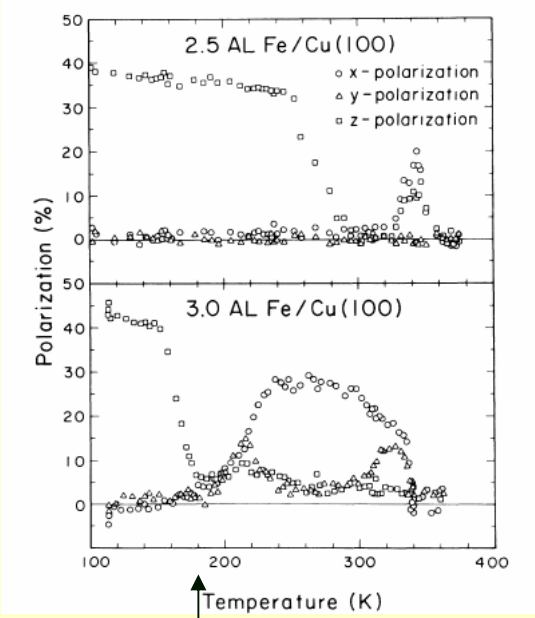

gap

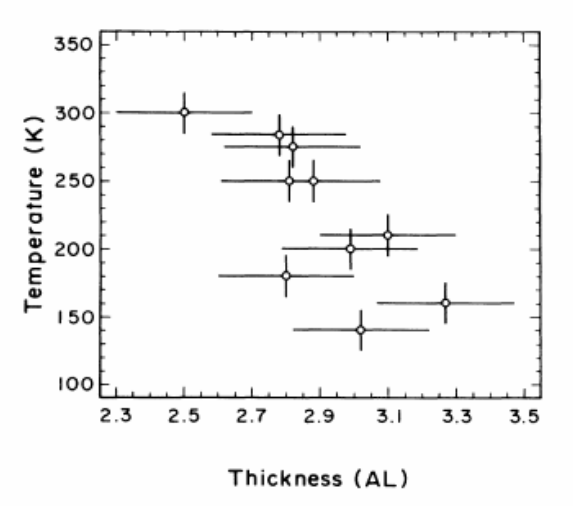

VOLUME 69, NUMBER 23 PHYSICAL REVIEW LETTERS 7 DECEMBER 1992

Magnetization Direction Switching in Fe/Cu(100) Epitaxial Films: Temperature and Thickness Dependence

R. Allenspach and A. Bischof
IBM Research Division, Zurich Research Laboratory, 8803 Rüschlikon, Switzerland
(Received 17 September 1992)

Scanning Electron Microscopy with Polarization Analysis (SEMPA)

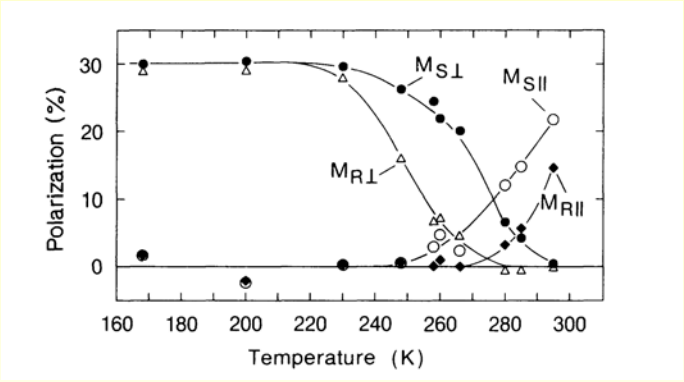

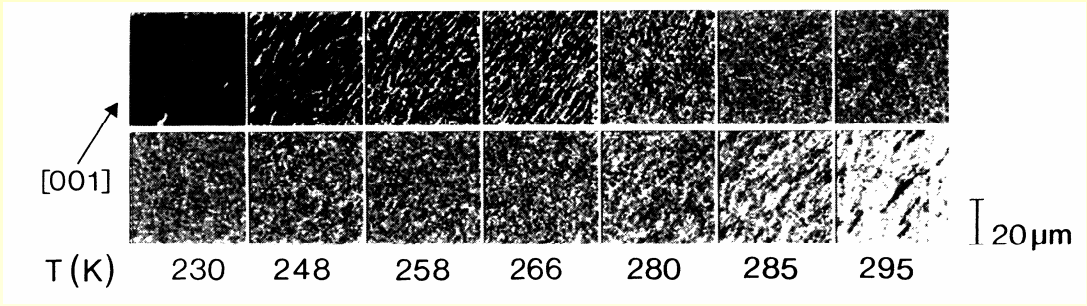

PHYSICAL REVIEW B 71, 224429 (2005)

Magnetic stripe melting at the spin reorientation transition in Fe/Ni/Cu(001)

C. Won,[1] Y. Z. Wu,[1] J. Choi,[1] W. Kim,[1,2] A. Scholl,[3] A. Doran,[3] T. Owens,[1] J. Wu,[1] X. F. Jin,[4,5] H. W. Zhao,[5] and Z. Q. Qiu[1]

Photoemision Electron Microscopy (PEEM)

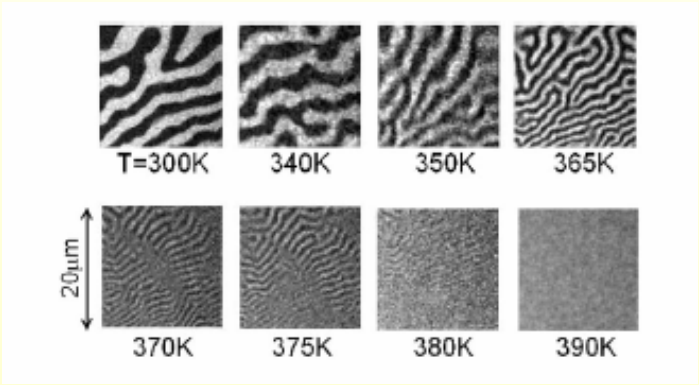

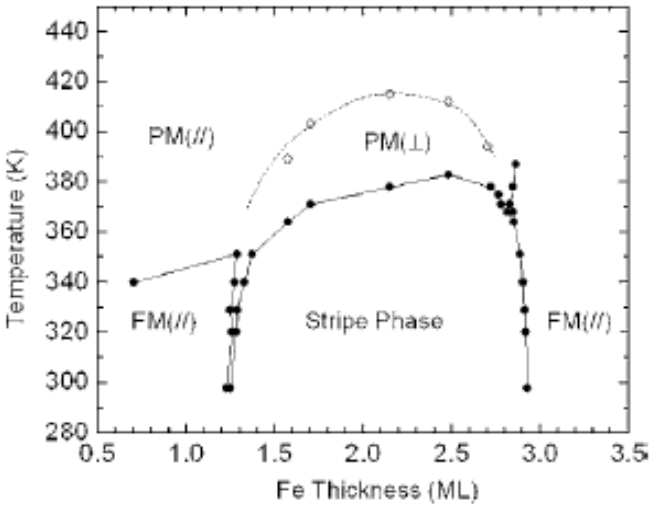

FIG. 5. Magnetic phase diagram of Fe/Ni(5.4 ML)/Cu(001).

Muestras crecidas a temperatura ambiente (~ 315 K): ausencia de TR para $\Delta \leq 5$ ML

Fe on Cu(100) - SEMPA

VOLUME 84, NUMBER 10 PHYSICAL REVIEW LETTERS 6 MARCH 2000

Two-Step Disordering of Perpendicularly Magnetized Ultrathin Films

A. Vaterlaus,[1] C. Stamm,[1] U. Maier,[1] M. G. Pini,[2] P. Politi,[3] and D. Pescia[1]
[1]*Laboratorium für Festkörperphysik, Eidgenössische Technische Hochschule Zürich, CH-8093 Zürich, Switzerland*
[2]*Istituto di Elettronica Quantistica, CNR, Via Panciatichi 56/30, I-50127 Firenze, Italy*
[3]*INFM, Unita di Firenze, Largo Enrico Fermi 2, I-50127 Firenze and Fachbereich Physik, Universität GH Essen, D-45117 Essen, Germany*
(Received 1 September 1999)

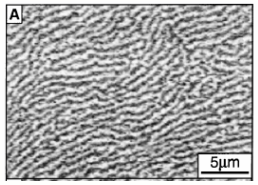

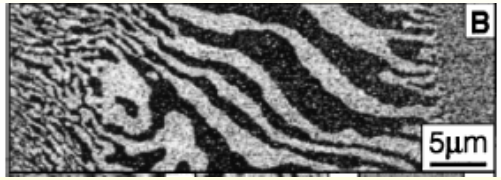

T = 200 K

Δ (ML) 4 1.6

Fe on Cu(100) - SEMPA

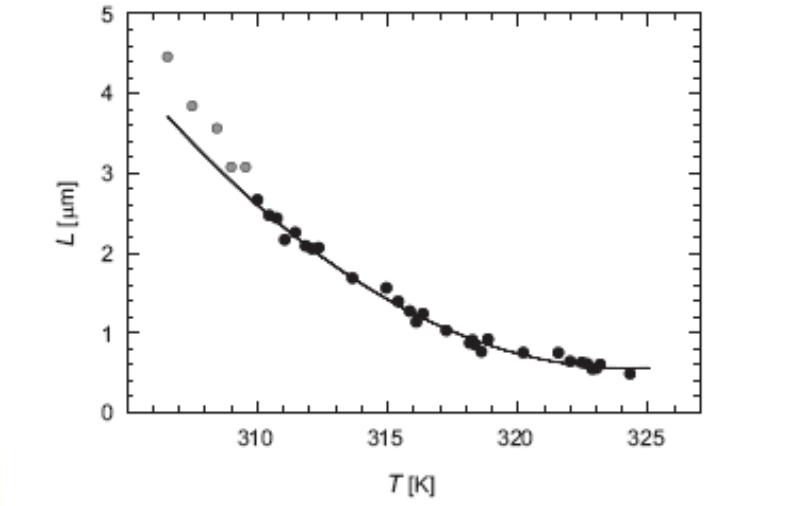

O. Portmann, A. Vaterlaus and D. Pescia,
Phys. Rev. Lett. **96**, 047212 (2006)

Fe/Ni(5ML)/Cu(100) - PEEM

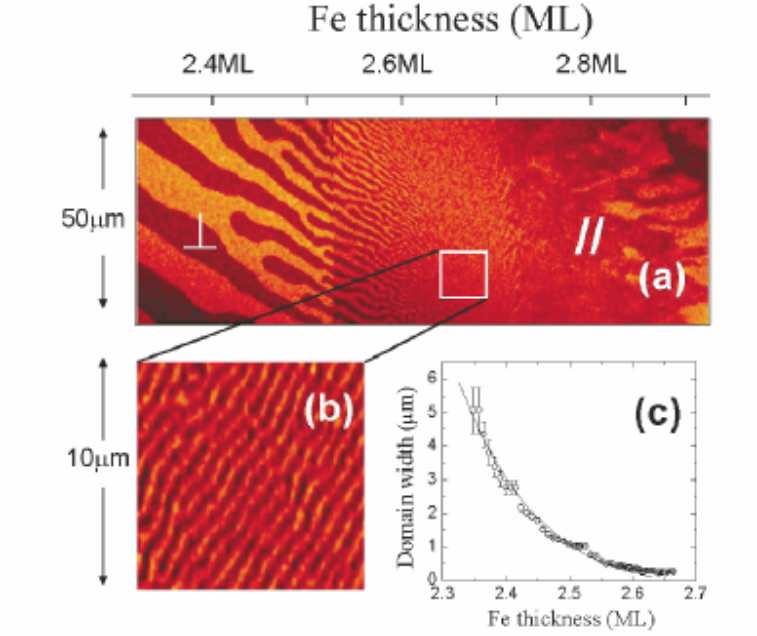

Y.Z. Wu et al, Phys. Rev. Lett. **93**, 117205 (2004)

Hamiltoniano de Heisenberg Clásico

$$H = H_{ex} + H_{dip} + H_{an}$$

intercambio: $$H_{ex} = -\delta \sum_{<i,j>} \boldsymbol{\sigma}_i . \boldsymbol{\sigma}_j$$

dipolar: $$H_{dip} = \sum_{(i,j)} \left(\frac{\boldsymbol{\sigma}_i . \boldsymbol{\sigma}_j}{r_{ij}^3} - 3 \frac{(\boldsymbol{\sigma}_i . \mathbf{r}_{ij})(\boldsymbol{\sigma}_j . \mathbf{r}_{ij})}{r_{ij}^5} \right)$$

Anisotropía superficial de sitio: $$H_{an} = -\eta \sum_i {}^{*} \left(\sigma_i^z\right)^2$$

$\boldsymbol{\sigma}_i$: spines clásicos

$|\boldsymbol{\sigma}_i| = 1$

$<i,j>$: suma sobre 1ros vecinos

(i,j): suma todos los pares $i\ j$

$\mathbf{r}_{ij}$: distancia entre $i\ j$

Límite $\eta \to \infty$ para una monocapa $\to$ Ising con interacciones competitivas:

$$H = -\delta \sum_{<i,j>} \sigma_i \sigma_j + \sum_{(i,j)} \frac{\sigma_i \sigma_j}{r_{ij}^3} \qquad \sigma_i = \pm 1$$

Ising:

$$H = -\delta \sum_{<i,j>} \sigma_i \, \sigma_j + \sum_{(i,j)} \frac{\sigma_i \, \sigma_j}{r_{ij}^3}$$

Estado fundamental en red cuadrada:

(Riguroso: Giuliani, Lebowitz & Lieb, Phys. Rev. B **74**, 064420 (2006))

Stripes de ancho $h(\delta)$ con $h(\delta) \sim e^{\delta/2}$ para $\delta >> 1$

A.B. MacIsaac *et al*, Phys. Rev. B **51**, 16033 (1995)

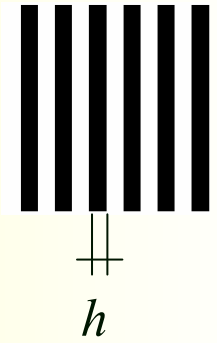

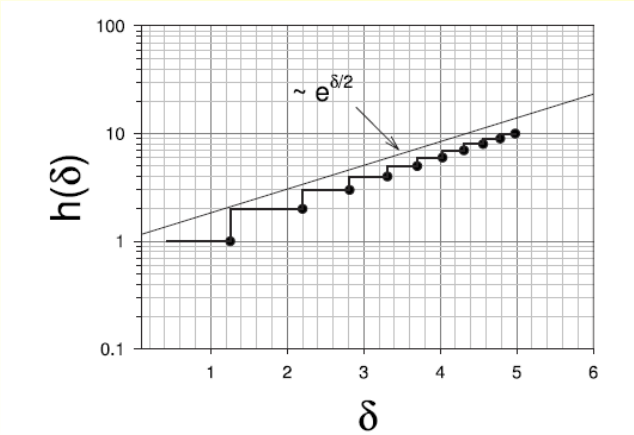

Heisenberg:

$$H = -\delta \sum_{<i,j>} \boldsymbol{\sigma}_i . \boldsymbol{\sigma}_j + \sum_{(i,j)} \left(\frac{\boldsymbol{\sigma}_i . \boldsymbol{\sigma}_j}{r_{ij}^3} - 3 \frac{(\boldsymbol{\sigma}_i . \mathbf{r}_{ij})(\boldsymbol{\sigma}_j . \mathbf{r}_{ij})}{r_{ij}^5} \right) - \eta \sum_i \left(\sigma_i^z \right)^2$$

Estado fundamental en red cuadrada:

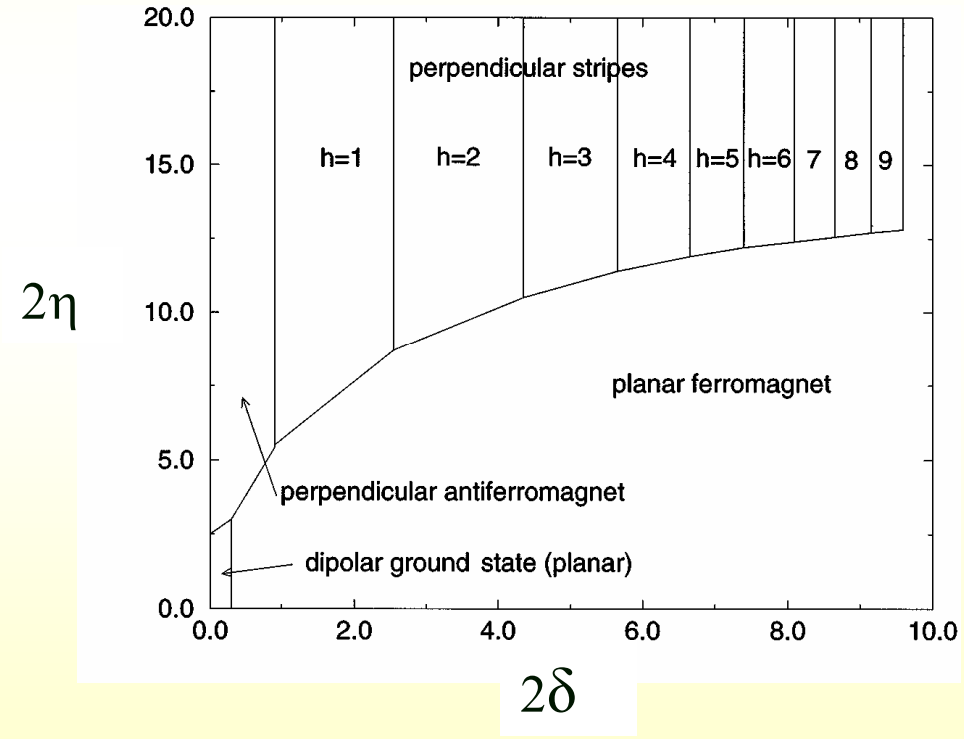

← Límite Ising

A.B. MacIsaac, K. De'Bell and J.P. Whitehead, Phys. Rev. Lett. 80, 616 (1998)

Heisenberg model:

$$H = -\delta \sum_{<i,j>} \boldsymbol{\sigma}_i . \boldsymbol{\sigma}_j + \sum_{(i,j)} \left(\frac{\boldsymbol{\sigma}_i . \boldsymbol{\sigma}_j}{r_{ij}^3} - 3 \frac{(\boldsymbol{\sigma}_i . \mathbf{r}_{ij})(\boldsymbol{\sigma}_j . \mathbf{r}_{ij})}{r_{ij}^5} \right) - \eta \sum_i \left(\sigma_i^z \right)^2$$

Finite temperature (MC):

A.B. MacIsaac, K. De'Bell and J.P. Whitehead,

Phys. Rev. Lett. 80, 616 (1998)

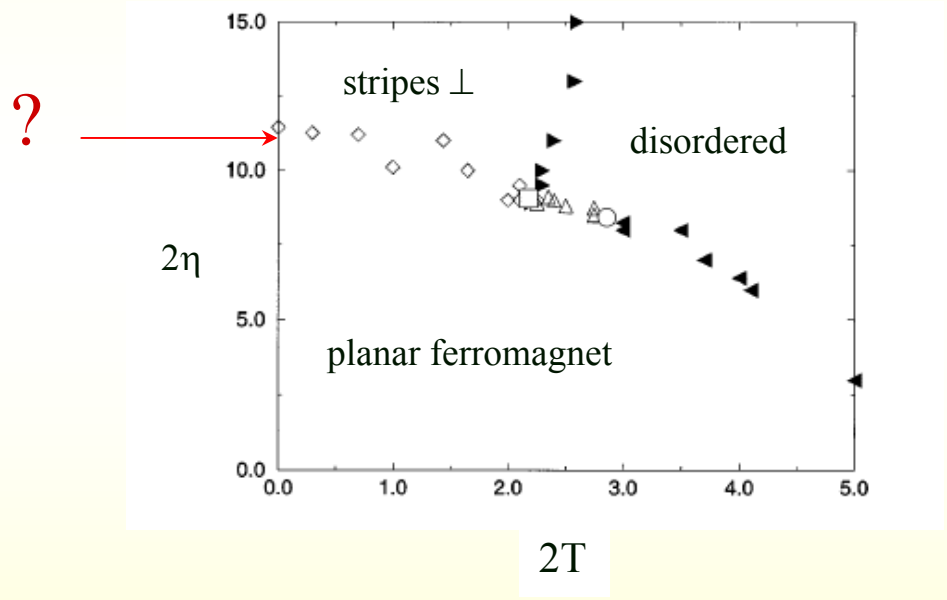

$\delta = 3$ $h(T=0,\eta\rightarrow\infty) = 4$

$L = 32$

At variance with theory and experiments

Heisenberg: diagrama de fases a T finita

Simulaciones de Monte Carlo en redes cuadradas de L x L sitios con condiciones de contorno periódicas

$L = 40 - \delta = 3$

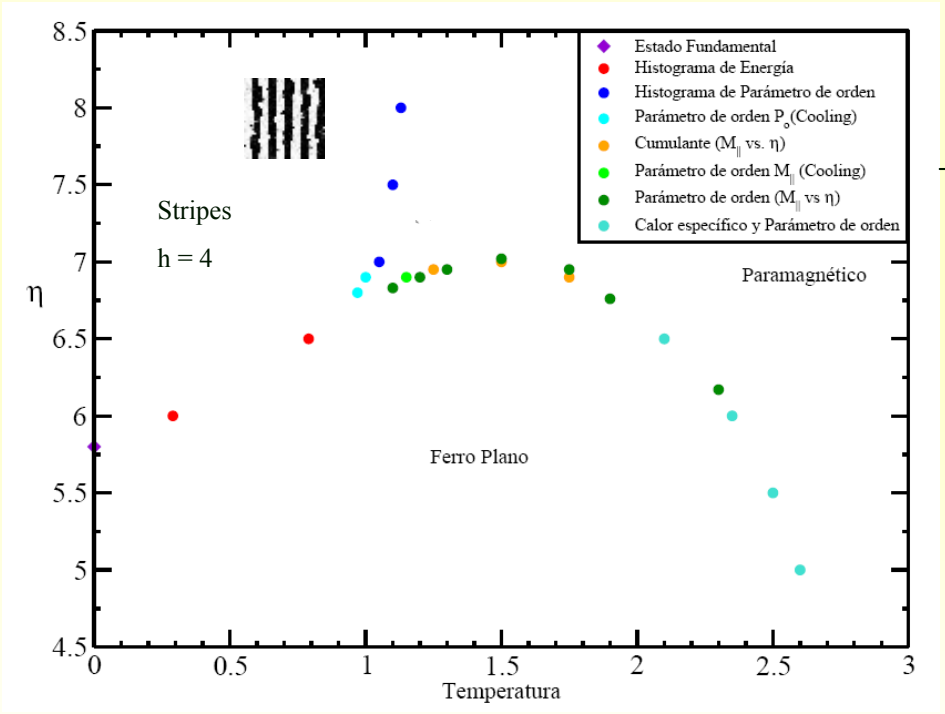

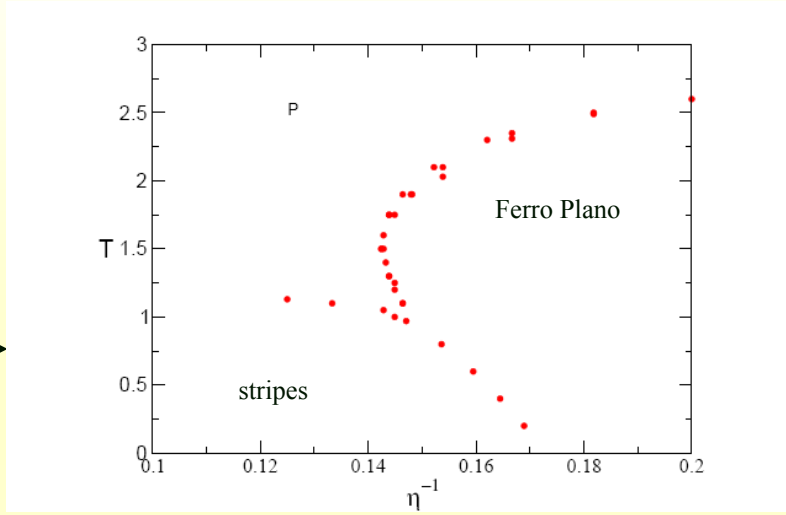

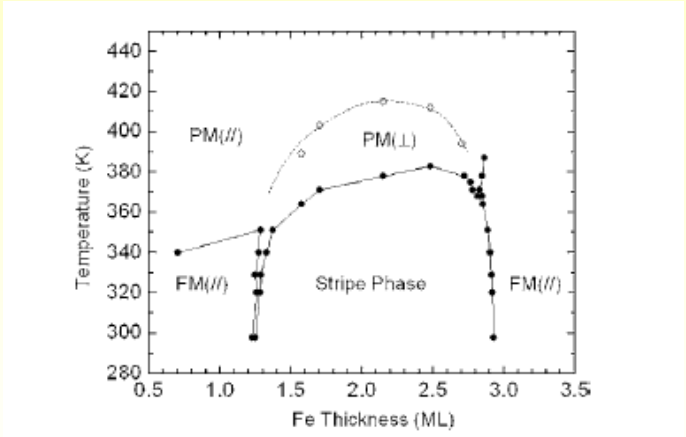

FIG. 5. Magnetic phase diagram of Fe/Ni(5.4 ML)/Cu(001).

M. Carubelli, S.A. Pighin, O.V. Billoni, F.A: Tamarit, D. A. Stariolo and S. A. Cannas, Phys. Rev. B **77**, 134417 (2008)

C. Won et al, Phys. Rev B **71**, 224429 (2005)

Orden de las transiciones

L = 40 - δ = 3

1er orden?

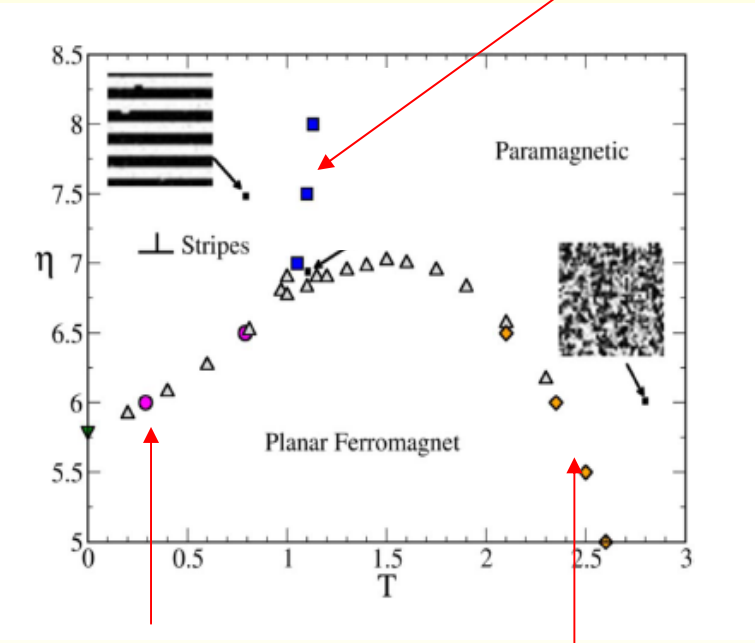

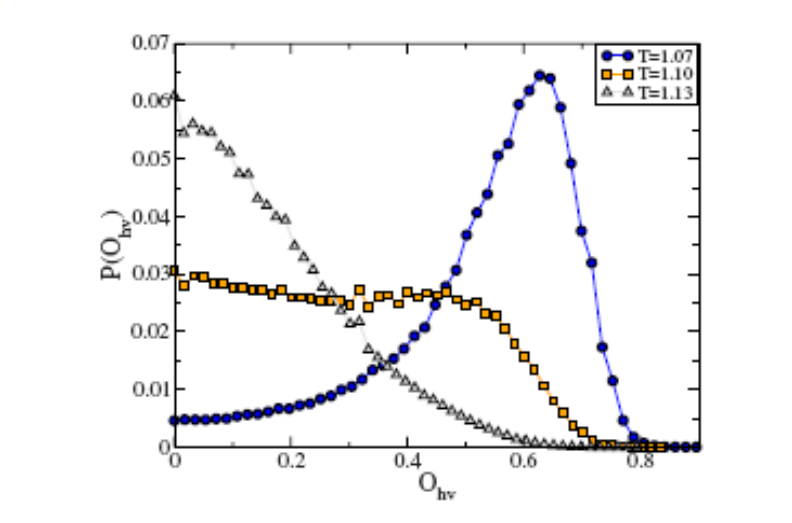

1er orden

2do orden? KT?

M. Carubelli, S.A. Pighin, O.V. Billoni, F.A: Tamarit, D. A. Stariolo and S. A. Cannas, Phys. Rev. B **77**, 134417 (2008)

Transición stripes → paramagneto: límite $\eta \to \infty$

K2APS Theory: Two dimensional solid of stripe domain walls

A. B. Kashuba and V.L Pokrovsky, PRB **48,** 10335 (1991)

A. Abanov, V. Kalatsky, V.L. Pokrovsky & W.M. Saslow, PRB **51**, 1023 (1995).

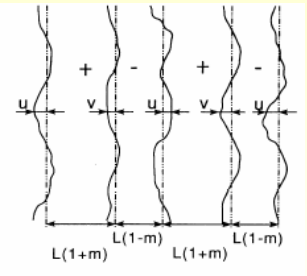

Fase desordenada → Líquido tetragonal

Dos escenarios posibles:

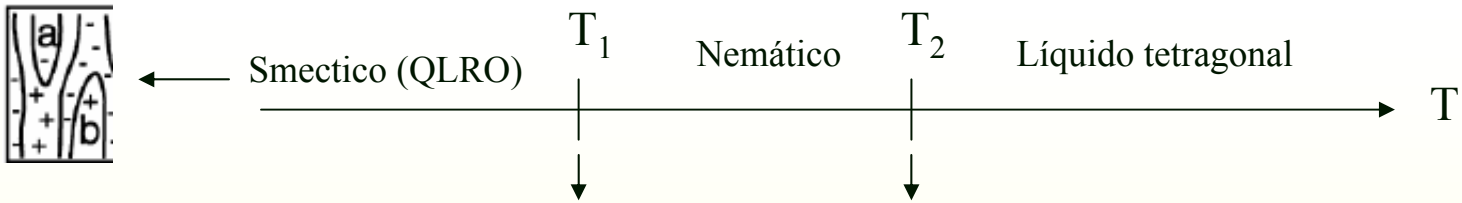

Kosterlitz-Thouless (KT) 2nd Order

ó

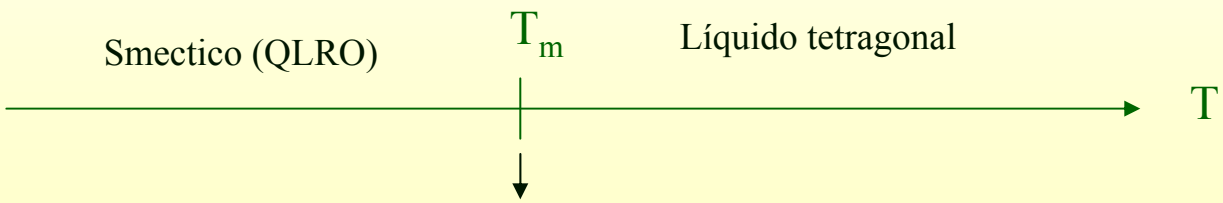

1st Order

Simulaciones de Monte Carlo (limite Ising): líquido tetragonal

Booth, A. B. MacIsaac, J. P. Whitehead and K. De'Bell, Phys. Rev. Lett. **75**, 950 (1995)

Static structure factor $S(\mathbf{k}) = \left\langle \left| \sigma_{\mathbf{k}} \right|^2 \right\rangle$

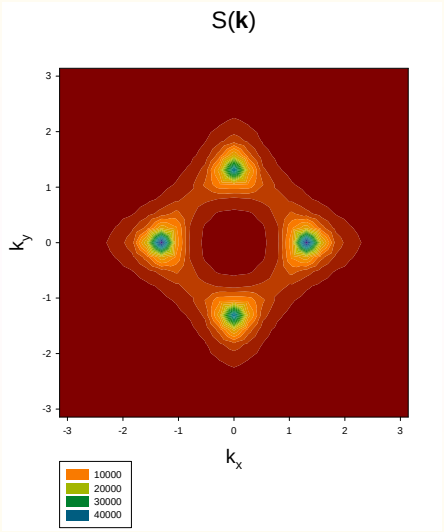

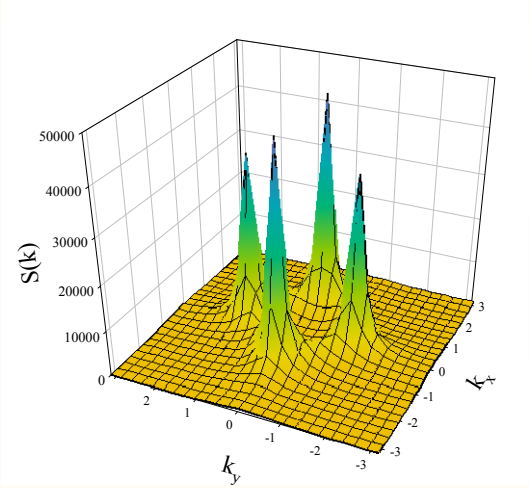

$\delta = 3$ L=64

T = 1 T = 1.5 T = 2.5 T = 4

Fe en Cu (SEMPA)

Cu(100)

Sustrato escalonado

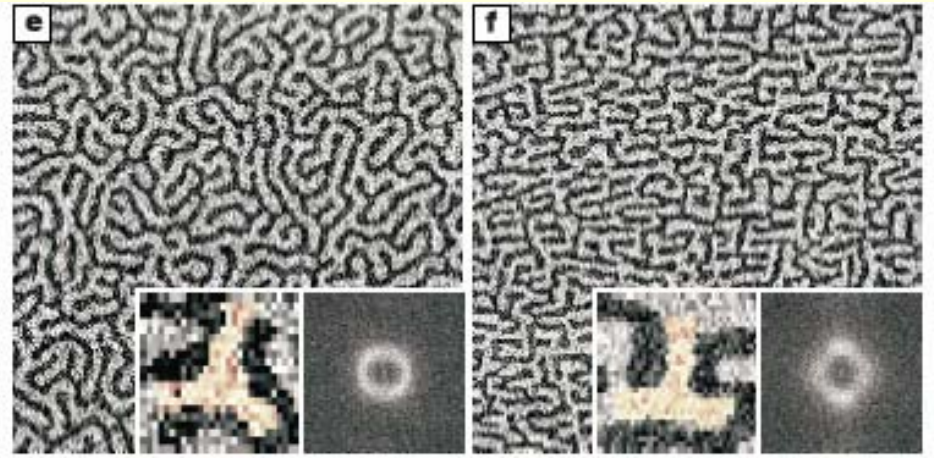

O. Portman, A. Vateriaus and D. Pescia, Nature **422**, 701 (2003).

Heisenberg

M. Carubelli, S.A. Pighin, O.V. Billoni, F.A: Tamarit,

D. A. Stariolo and S. A. Cannas, Phys. PRB **77**, 134417 (2008)

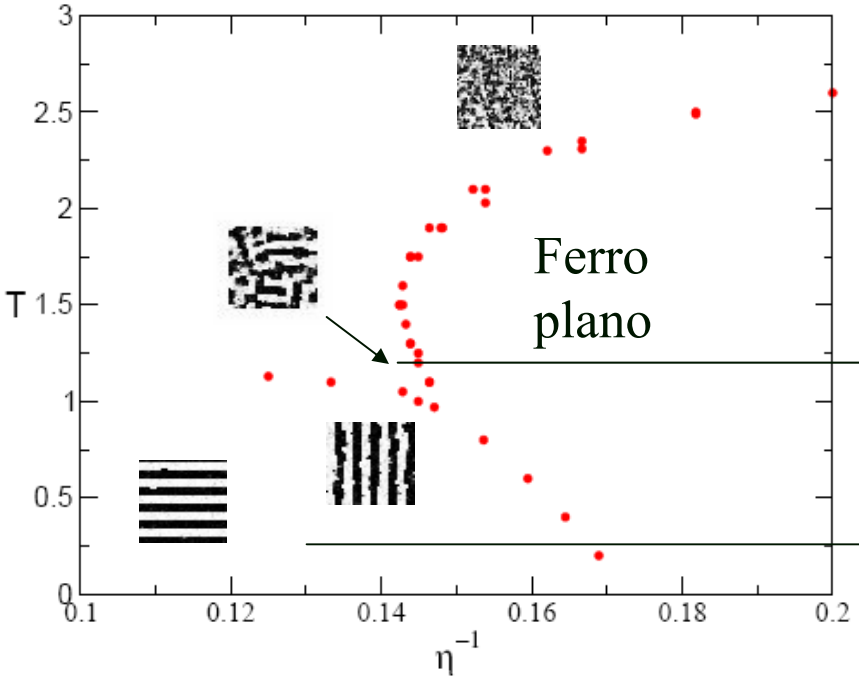

$$\overline{m_\tau}(\vec{r}) \equiv \frac{1}{\tau}\sum_{t=1}^{\tau} S^z(\vec{r},t)$$

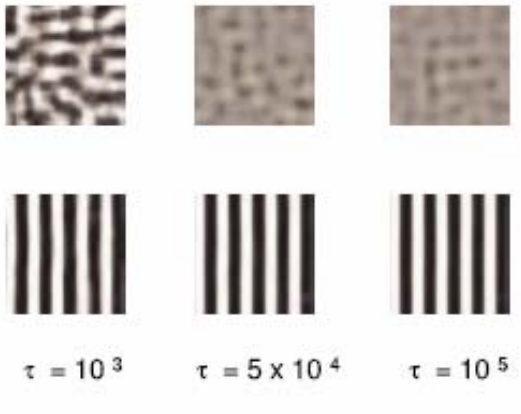

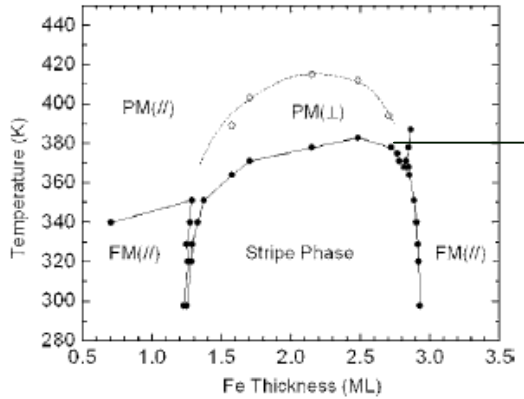

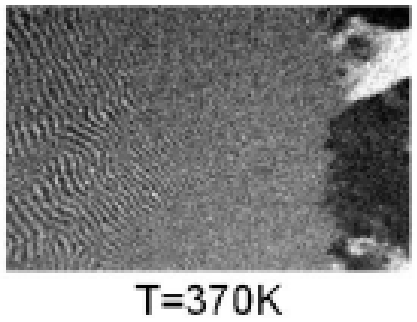

FIG. 5. Magnetic phase diagram of Fe/Ni(5.4 ML)/Cu(001).

C. Won et al, PRB **71**, 224429 (2005)

Simulaciones de Monte Carlo (limite Ising): fase nemática

S. A. Cannas, M. F. Michelon, D. A. Stariolo and F. A. Tamarit, Phys. Rev. B. **73**, 184425 (2006)

$$C_x(r) \equiv \frac{1}{N}\sum_{x,y}\langle \sigma_{x,y}\ \sigma_{x+r,y}\rangle$$

$$C_y(r) \equiv \frac{1}{N}\sum_{x,y}\langle \sigma_{x,y}\ \sigma_{x,y+r}\rangle$$

$\delta = 2$

L = 92 – T = 0.78

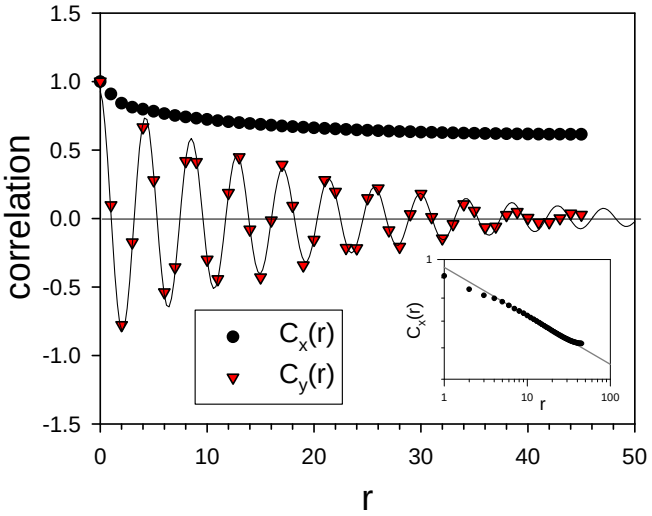

Fit: $C(r) = A\ sen(k_0 r + \phi)\ e^{-r/\xi}$

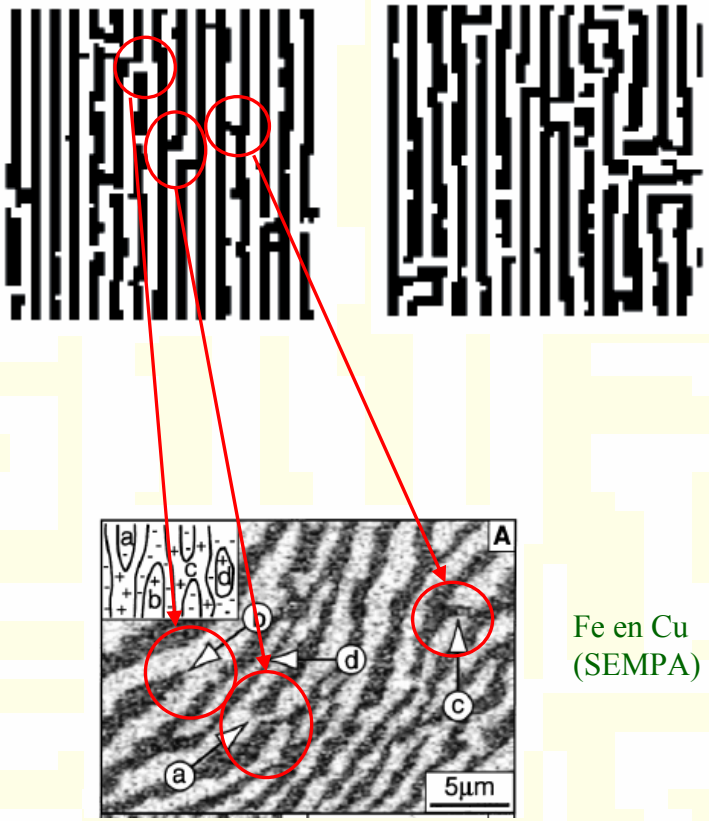

Fe en Cu (SEMPA)

A. Vaterlaus et al, PRL 84, 2247 (2000).

Diagrama de fases a T finita (limite Ising)

S. A. Pighin and S. A. Cannas, Phys. Rev. B. **75**, 224433 (2007)

Monte Carlo: L ~ 60

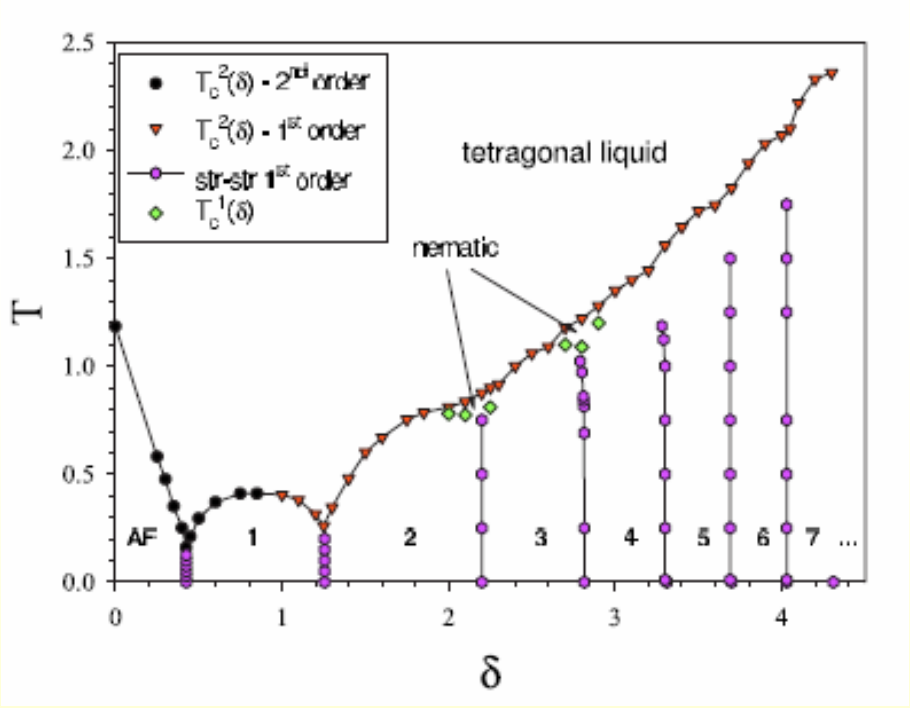

Campo medio

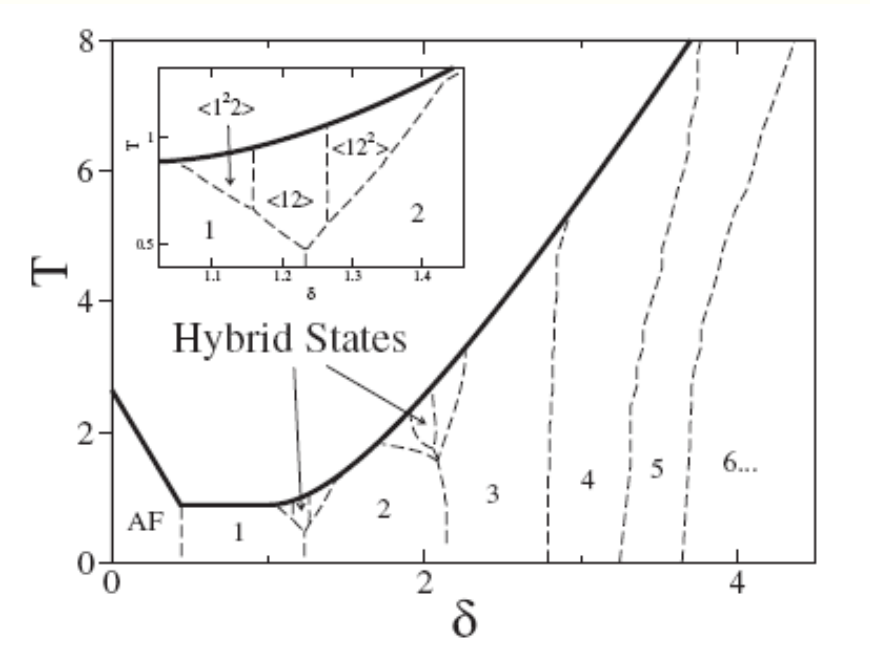

K2APS: ambos escenarios se cumplen

Transiciones stripes-nematic y nematic-tetragonal

S. A. Cannas, et al, Phys. Rev. B. **73**, 184425 (2006)

E. Rastelli et al, Phys. Rev. B. **73**, 144418 (2006)

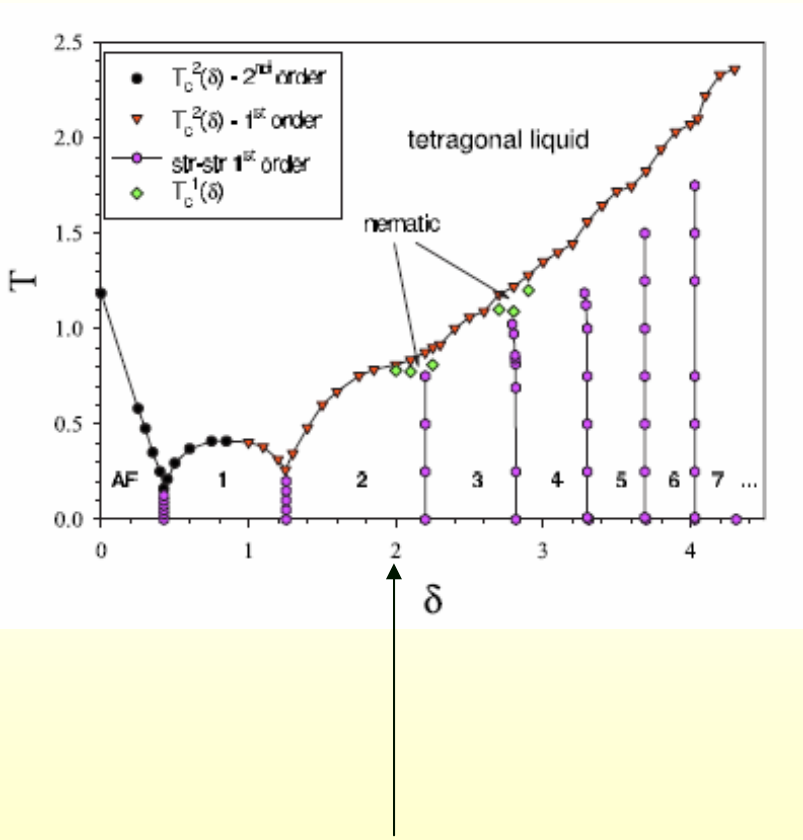

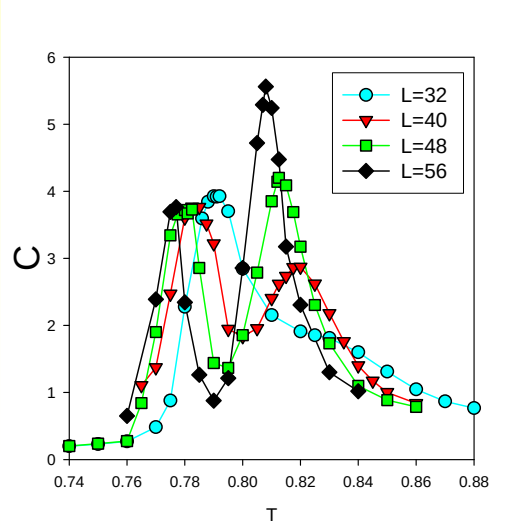

$\delta = 2$

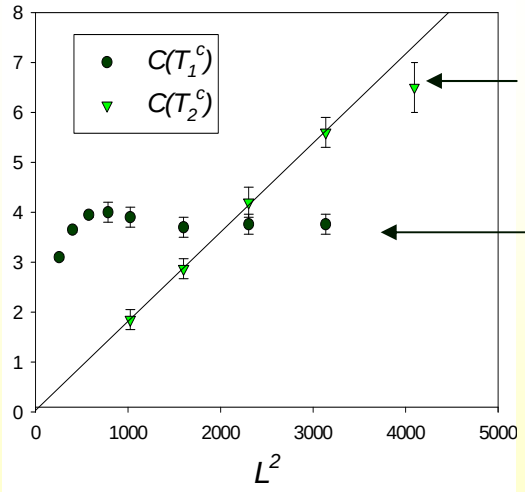

$C|_{max}(T_2) \sim L^2$

1^{st} order

KT ?

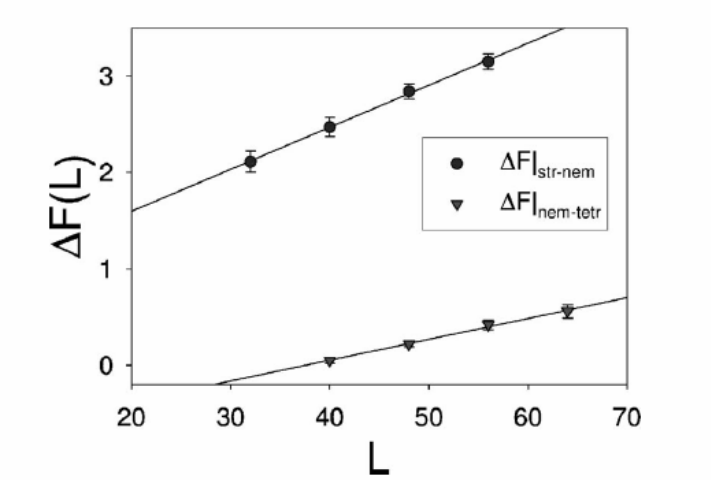

S. A. Cannas, M. F. Michelon, D. A. Stariolo and F. A. Tamarit, Phys. Rev. B. **73**, 184425 (2006)

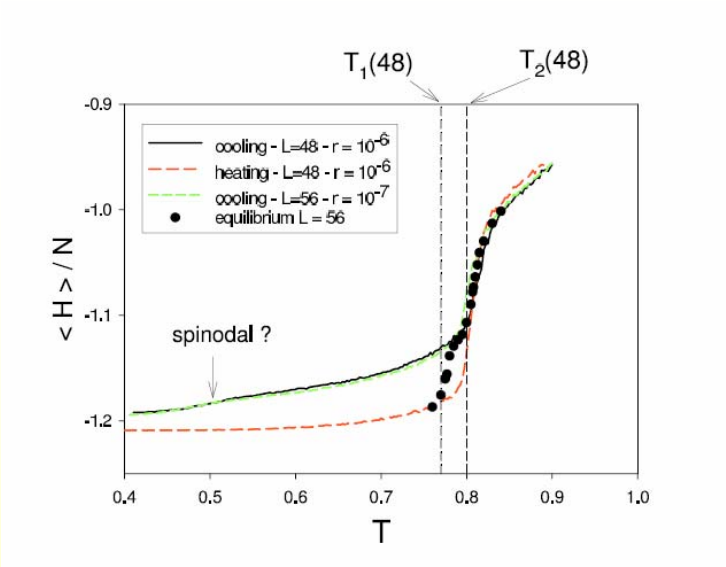

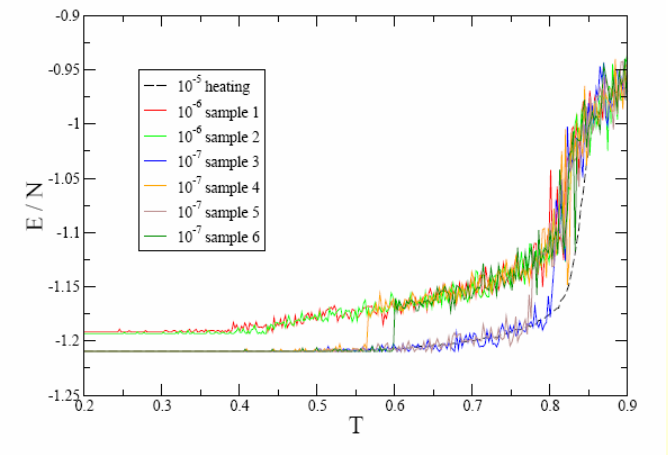

S. A. Cannas, M. F. Michelon, D. A. Stariolo and F. A. Tamarit, Phys. Rev. E **78**, 051602 (2008)

Landau-Ginzburg Model

$$H_0[\phi] = \frac{1}{2}\int d^2r\left[\left(\nabla\phi(\mathbf{r})\right)^2 + r_0\phi^2(\mathbf{r}) + \frac{u}{2}\phi^4(\mathbf{r})\right] + \frac{1}{2\delta}\int d^2r\int d^2r'\,\frac{\phi(\mathbf{r})\phi(\mathbf{r}')}{\left|\mathbf{r}-\mathbf{r}'\right|^3}$$

$$r_0 = r_0(T)$$

$$Z = \int \mathcal{D}\phi\; e^{-H[\phi]/T} = e^{-F(T)/T}$$

$$H_0[\phi] = \frac{1}{2}\int d^2r\left[\left(\nabla\phi(\mathbf{r})\right)^2 + r_0\phi^2(\mathbf{r}) + \frac{u}{2}\phi^4(\mathbf{r})\right] + \frac{1}{2\delta}\int d^2r\int d^2r'\frac{\phi(\mathbf{r})\phi(\mathbf{r}')}{|\mathbf{r}-\mathbf{r}'|^3}$$

Campo medio: $\rightarrow$ transición paramagneto – fase modulada

$$\frac{\delta H[\phi(\mathbf{r})]}{\delta\phi(\mathbf{r})} = -\nabla^2\phi(\mathbf{r}) + r_0\phi(\mathbf{r}) + u\phi^3(\mathbf{r}) + \frac{1}{\delta}\int d^2\mathbf{r}'\frac{\phi(\mathbf{r}')}{|\mathbf{r}-\mathbf{r}'|^3} = 0$$

T. Garel and S. Doniach,

Phys. Rev. B. **26**, 325 (1982)

$$\phi(r) = m_{k_m}\cos\left(\mathbf{k}_m.\mathbf{r}\right) \qquad k_m = k_m(\delta)$$

- transición de 2do orden

Aproximación de Hartree autoconsistente: $\rightarrow \quad \phi^4(\mathbf{r}) \quad \rightarrow \quad \phi^2(\mathbf{r})\left\langle\phi^2(\mathbf{r})\right\rangle$

S. A. Cannas, D. A. Stariolo and F. A. Tamarit, Phys. Rev. B. **69**, 092409 (2004)

- transición de 1er orden (inducida por fluctuaciones)

Extended Landau-Ginzburg Model

D. G. Barci and D. A. Stariolo, Phys. Rev Lett., **98**, 200604 (2007)

RG: $H_0 \to H_0 + H_1$ $\qquad H_1[\phi] = \frac{u_2}{2}\int d^2r \ \mathrm{Tr}\, Q^2 \qquad Q_{ij}(\mathbf{r}) = \phi(\mathbf{r})\left(\nabla_i\nabla_j - \delta_{ij}\frac{1}{2}\nabla^2\right)\phi(\mathbf{r})$

Aproximación autoconsistente: $\to \quad \phi^4(\mathbf{r}) \quad \to \quad \phi^2(\mathbf{r})\langle\phi^2(\mathbf{r})\rangle$ Hartree

$$\mathrm{Tr}\, Q^2 \to \mathrm{Tr}\left\{\phi(\mathbf{r})\left(\nabla_i\nabla_j - \delta_{ij}\frac{1}{2}\nabla^2\right)\phi(\mathbf{r})\right\}\langle Q_{ij}(\mathbf{r})\rangle$$ MF

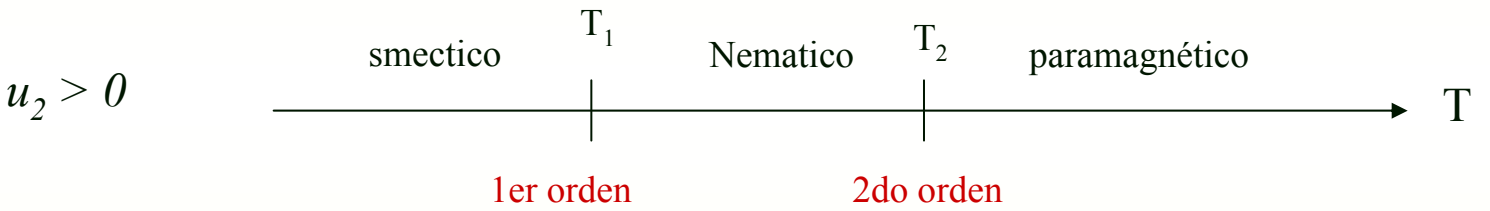

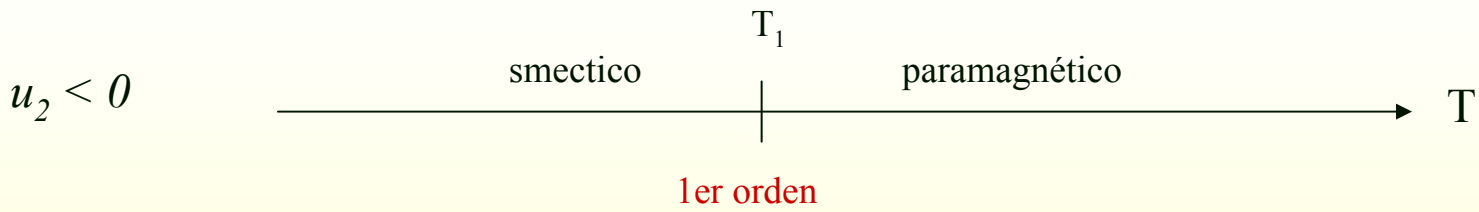

Fluctuaciones: D. G. Barci and D. A. Stariolo, arXiv: 0808.2494

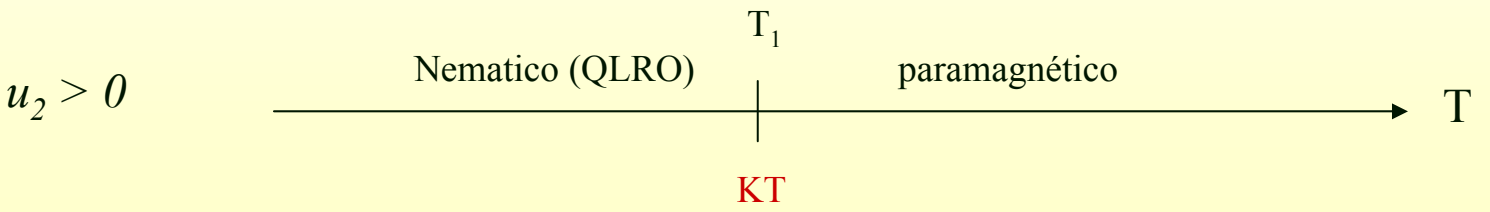

Simulaciones numéricas: Landau-Ginzburg + dinámica de Langevin

L. Nicolao and D. A. Stariolo, Phys. Rev. B **76**, 054453 (2007)

$$H_0[\phi] = \frac{1}{2}\int d^2r\left[(\nabla\phi(\mathbf{r}))^2 + r_0\phi^2(\mathbf{r}) + \frac{u}{2}\phi^4(\mathbf{r})\right] + \frac{1}{2\delta}\int d^2r\int d^2r' \frac{\phi(\mathbf{r})\phi(\mathbf{r}')}{|\mathbf{r}-\mathbf{r}'|^3}$$

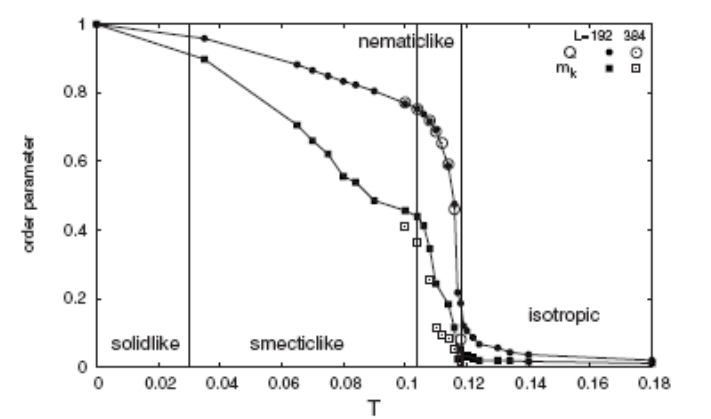

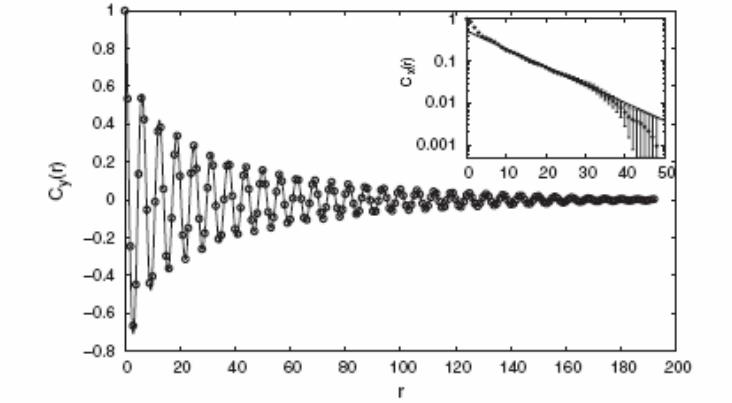

L - G

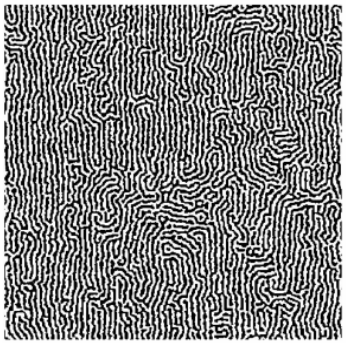

Ising

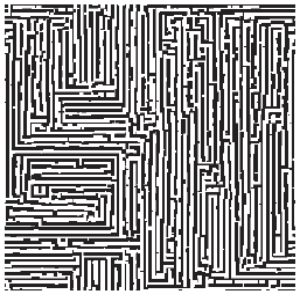

Fe on Cu

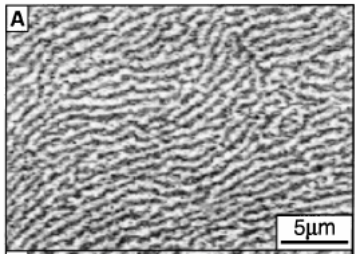

Dependencia del ancho de fajas con T (limite Ising)

Campo medio

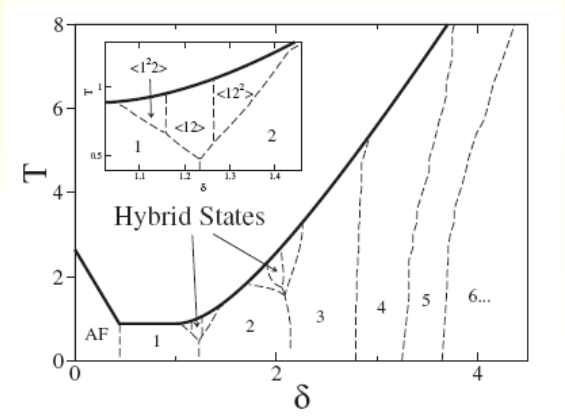

MC

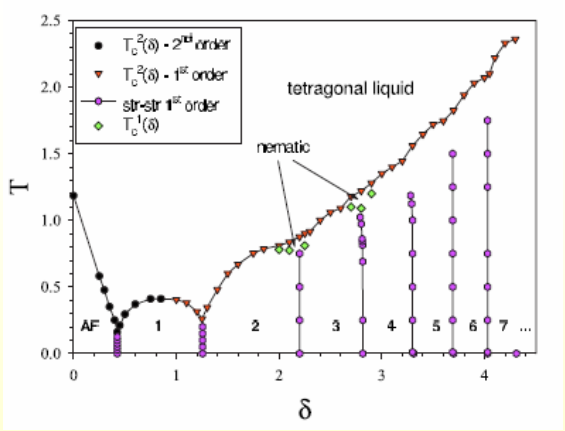

S. A. Pighin and S. A. Cannas,

Phys. Rev. B. **75**, 224433 (2007)

Campo medio

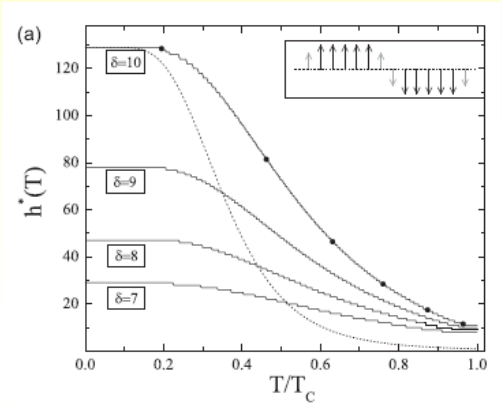

A. Vindigni, N. Saratz, O. Portmann, D. Pescia and P. Politi, Phys. Rev. B 77, 092414 (2008)

Fe on Cu(100) - SEMPA

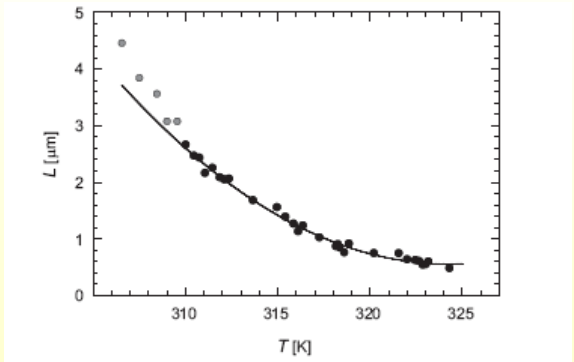

O. Portmann, A. Vaterlaus and D. Pescia, Phys. Rev. Lett. **96**, 047212 (2006)

Dependencia del ancho de fajas con η (~espesor^{-1})

Heisenberg - L = 144 – δ = 6 (*h(T=0) = 24*)

$$\eta = \eta_0 + r\,t$$

T = 0.5

r = 10^{-5}

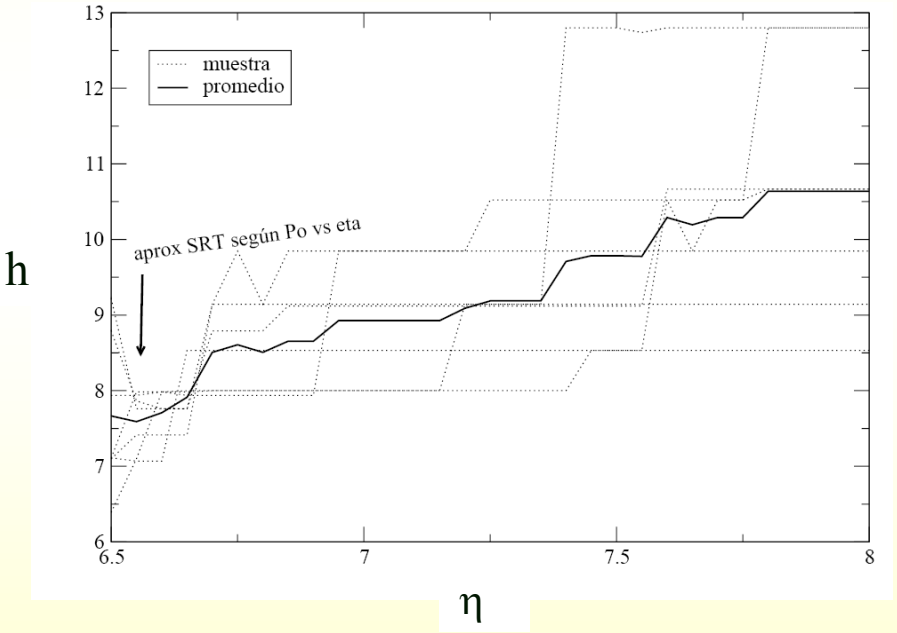

Heisenberg - L = 120 – δ = 6 – T = 0.5

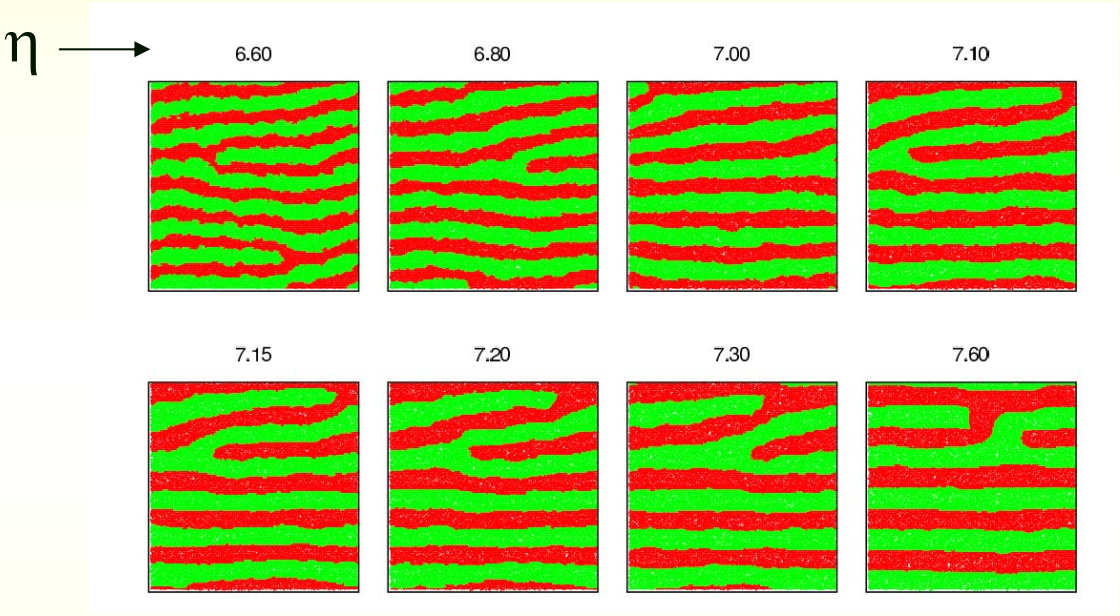

Fe on Cu(100) - SEMPA

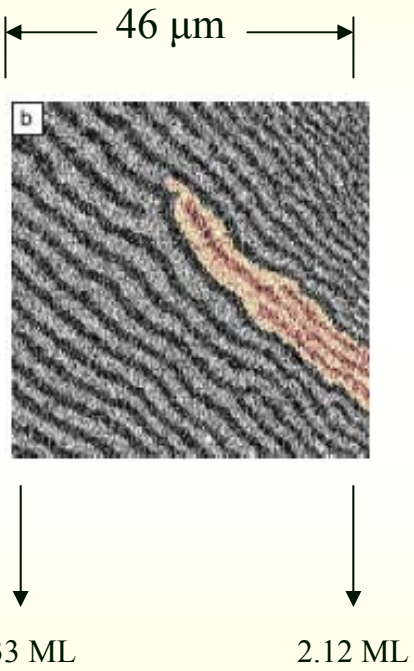

O. Portman, A. Vateriaus and D. Pescia, Nature **422**, 701 (2003).

Simulación de cuñas: $\Delta \sim \eta^{-1}$

$\delta = 6\ T = 0.5$

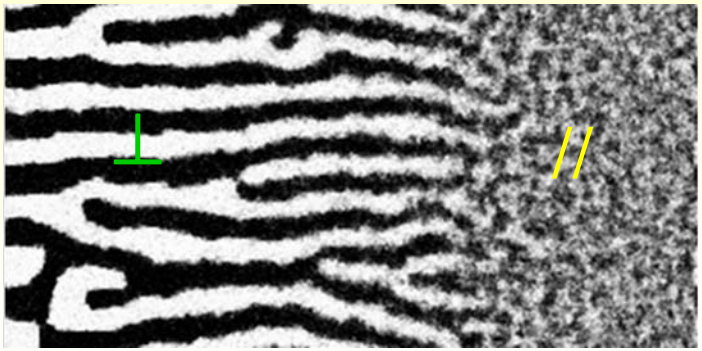

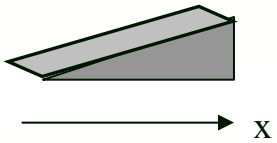

$\eta \sim 1/\Delta$

$\Delta = a + b\ x$

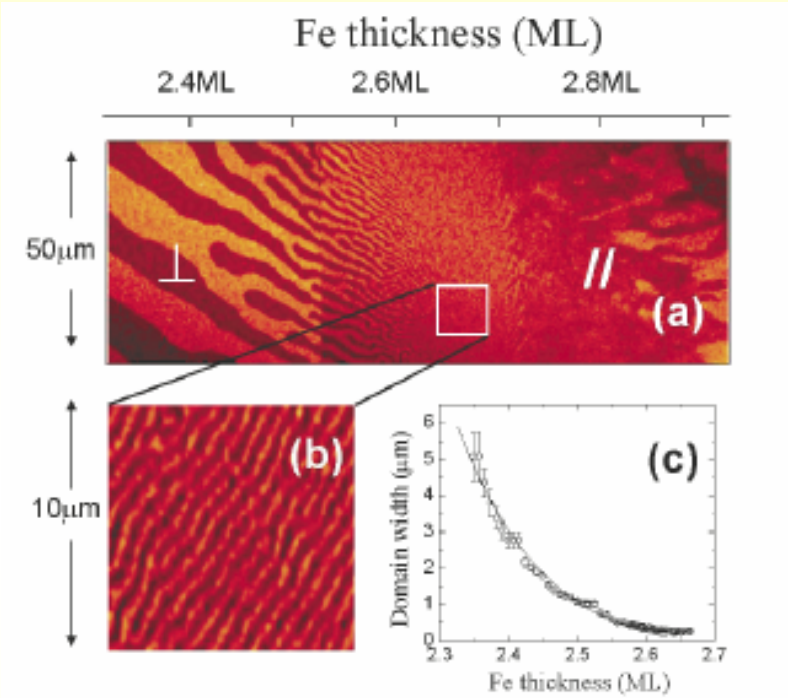

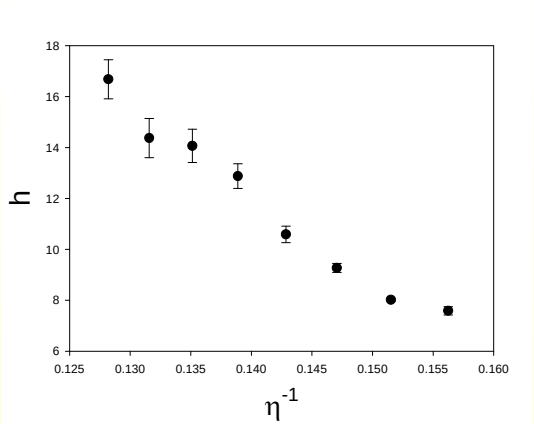

Y.Z. Wu et al, Phys. Rev. Lett. **93**, 117205 (2004)

Configuraciones “canted”

J. P. Whitehead, A. B. MacIsaac and K. De’Bell, Phys. Rev. B 174415 (2008)

$\delta = 4.45 - h(T=0,\eta\rightarrow\infty) = 8$

$L = 128$

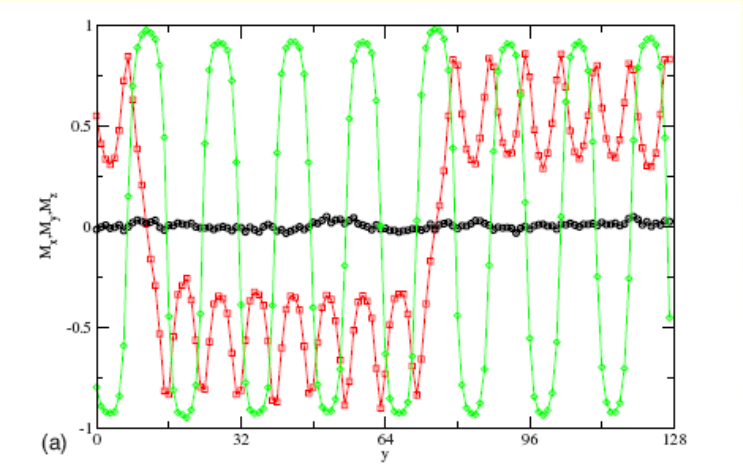

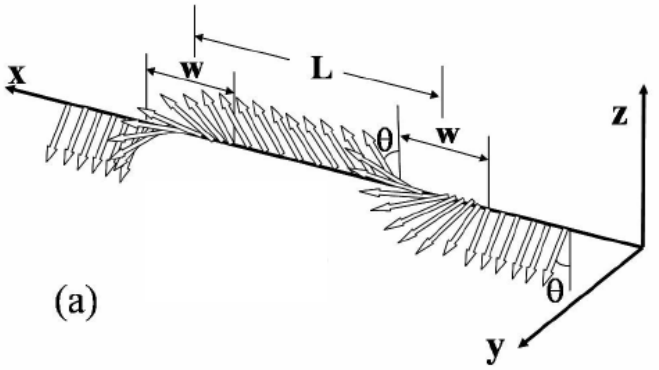

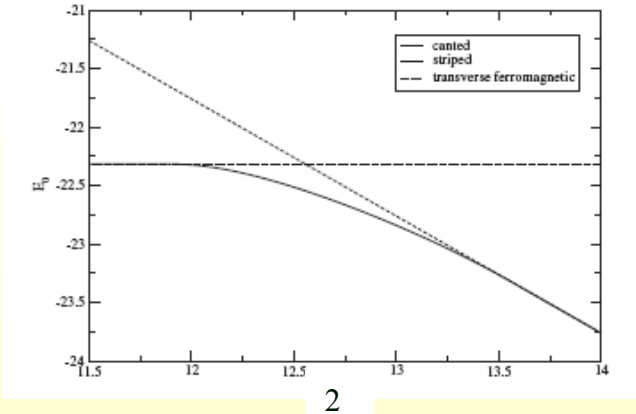

2

η

δ = 3 - L = 40

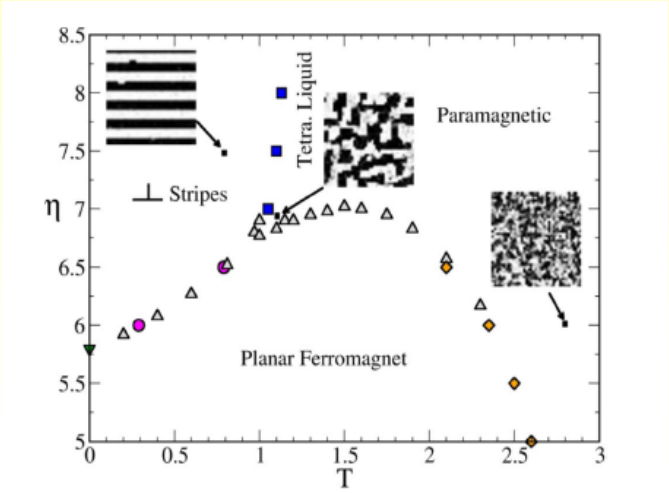

M. Carubelli, et al, Phys. Rev. B **77,** 134417 (2008)

δ= 4.45 - L = 128

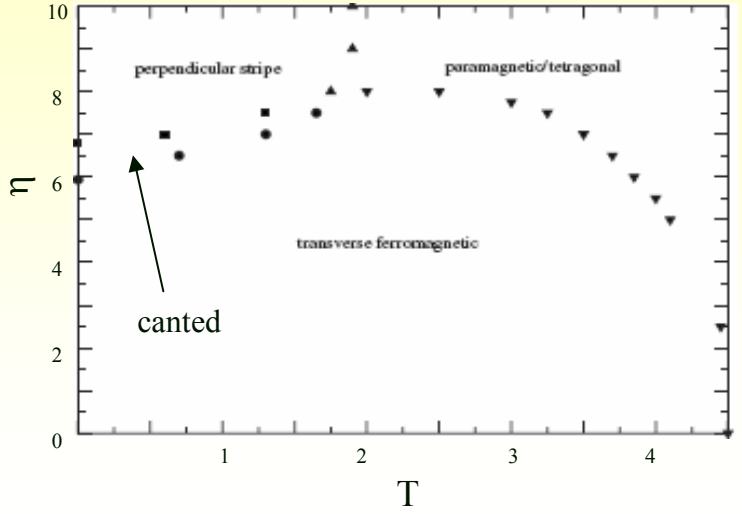

J. P. Whitehead, et al, Phys. Rev. B **77,** 174415 (2008)

δ= 6 - L = 120

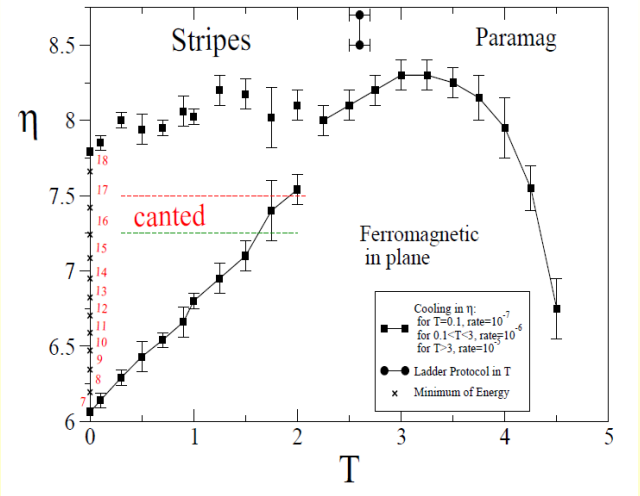

Diagrama de fases a T = 0:

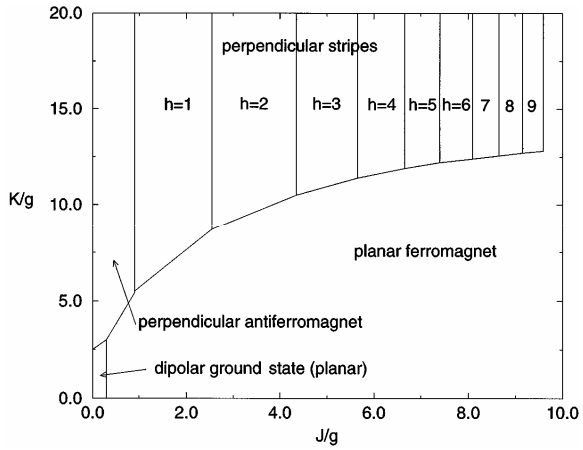

Teoría de Yafet & Giorgy:

$$\vec{S}_{(x,y)} = \vec{M}(x)\ \forall y$$

$$M^x(x) = 0\ \forall x$$

$$\mathcal{H} = -\delta \sum_{<i,j>} \vec{S}_i \cdot \vec{S}_j + \sum_{(i,j)} \left[\frac{\vec{S}_i \cdot \vec{S}_j}{r_{ij}^3} - 3\,\frac{(\vec{S}_i \cdot \vec{r}_{ij})\,(\vec{S}_j \cdot \vec{r}_{ij})}{r_{ij}^5} \right] - \eta \sum_i (S_i^z)^2$$

$$\downarrow$$

$$e\left[\vec{M}, \delta, \eta\right] = -(2g+\delta) - \frac{\delta}{L}\sum_x \vec{M}(x).\vec{M}(x+1) + \frac{1}{L}\sum_{x,x'} \frac{M^z(x)\,M^z(x')}{|x-x'|^2} - \frac{\kappa}{L}\sum_x \left[M^z(x)\right]^2$$

$$\kappa \equiv \eta - 3g + c$$

$$e\left[\vec{M},\delta,\eta\right] = -(2g+\delta) - \frac{\delta}{L}\sum_{x}\vec{M}(x).\vec{M}(x+1) + \frac{1}{L}\sum_{x,x'}\frac{M^z(x)\,M^z(x')}{|x-x'|^2} - \frac{\kappa}{L}\sum_{x}\left[M^z(x)\right]^2$$

Ansatz: perfil de magnetización

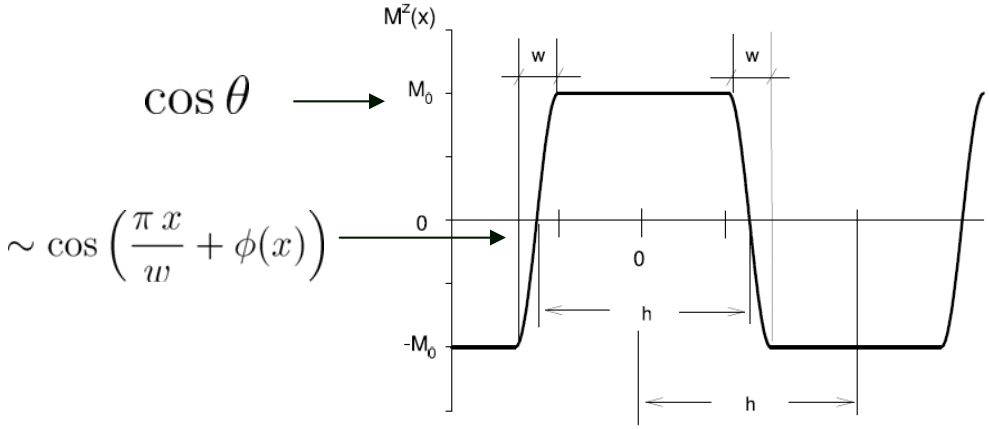

Solución "canted"

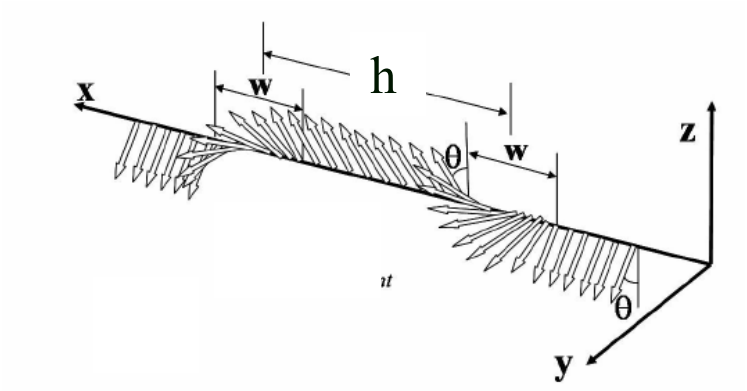

$\delta = 7.5$

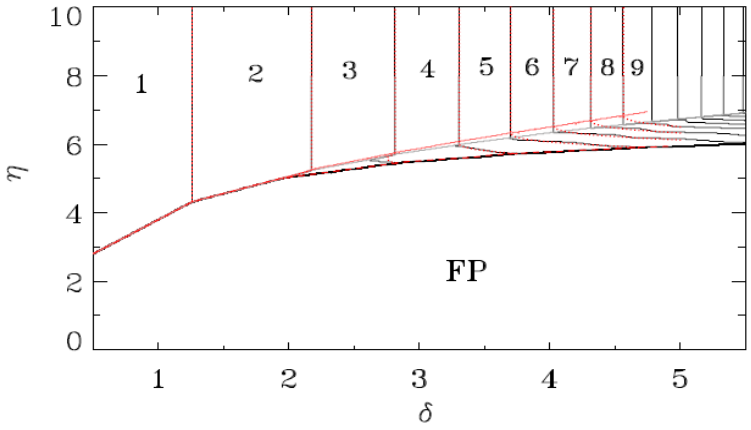

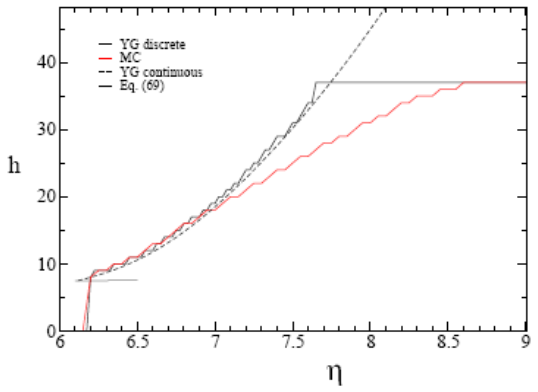

$\delta = 7.5$

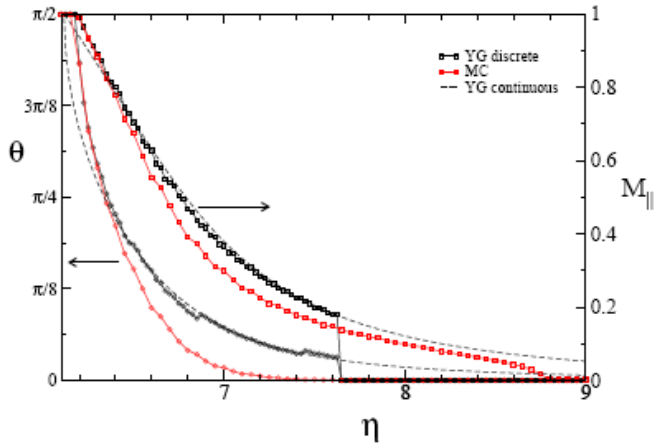

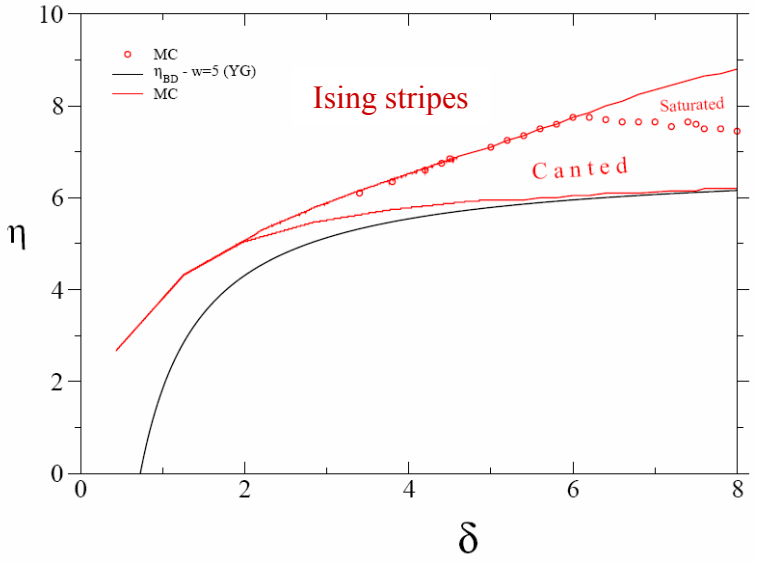

Efecto de campos magnéticos externos

Heisenberg: $\delta = 3$, $L = 40$, $\eta = 6.5$

H // al plano

H_y=0.1

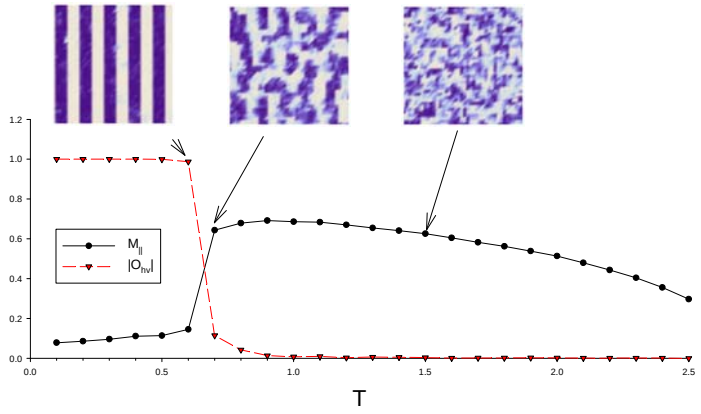

H_x=0.1

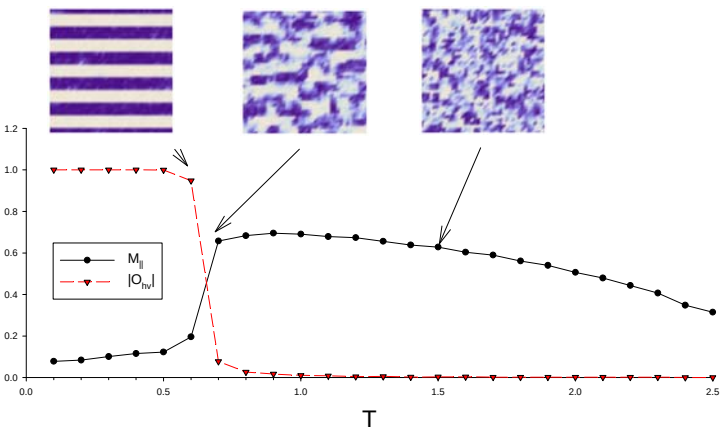

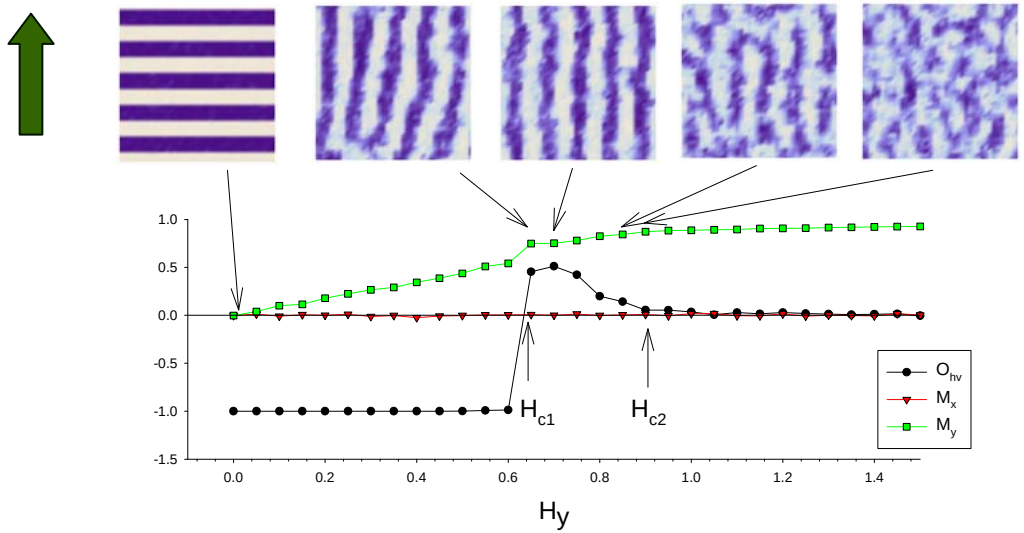

Efecto de campos magnéticos externos

H ⊥ al plano

- Campo medio (Landau-Ginzburg): T. Garel and S. Doniach, Phys. Rev. B 26, 325 (1982)

(i) the stripe solution,

$$m = m_{s0} + m_s \cos(q_0 x) \quad ;$$

(ii) the bubble solution,

$$m = m_{B0} + \sum_{i=1}^{3} m_B \cos(\vec{k} \cdot \vec{r}_i) \quad ,$$

with

$$\sum_{i=1}^{3} \vec{k}_i = 0, \quad |\vec{k}| = q_0 \quad .$$

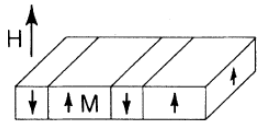

(a)

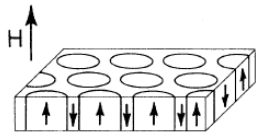

(b)

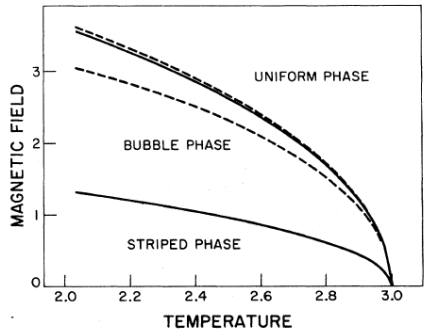

FIG. 2. Ginzburg-Landau phase diagram: solid lines, first-order phase boundaries; dashed lines, critical fields.

•Monte Carlo (Ising): J. Arlett et al, , Phys. Rev. B 54, 3394 (1996)

$L = 32 - \delta = 3$

T = 0.8 T = 1.5

H = 0

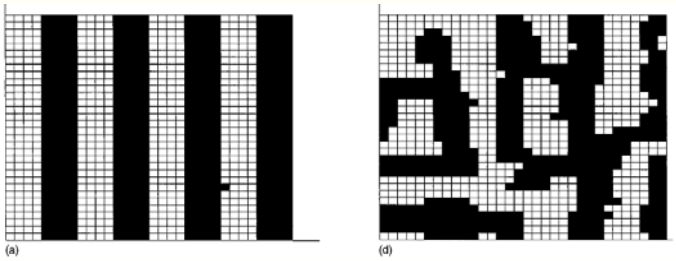

T = 0.865 T = 1.37

H = 1

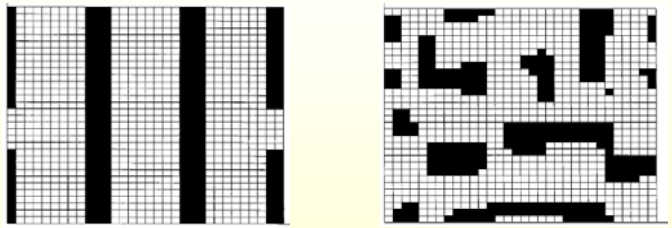

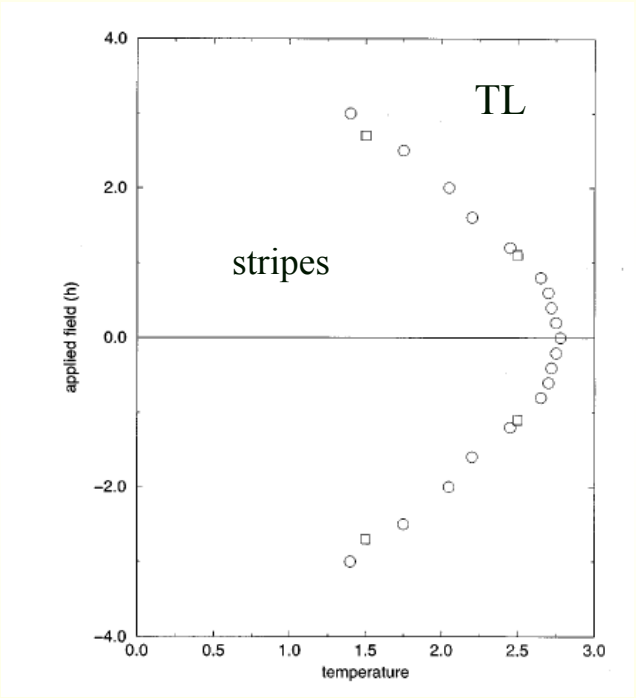

Magnetic Bubble Domain Phase at the Spin Reorientation Transition of Ultrathin Fe/Ni/Cu(001) Film

J. Choi,[1] J. Wu,[1] C. Won,[1,2] Y. Z. Wu,[1,3] A. Scholl,[4] A. Doran,[4] T. Owens,[1] and Z. Q. Qiu[1]

[1]*Department of Physics, University of California at Berkeley, Berkeley, California 94720, USA*

[2]*Department of Physics, Kyung Hee University, Seoul 130-701, Korea*

[3]*Surface Physics Laboratory (National Key Laboratory) and Advanced Material Laboratory, Fudan University, Shanghai 200433, China*

[4]*Advanced Light Source, Lawrence Berkeley National Laboratory, Berkeley, California 94720, USA*

(Received 8 June 2006; revised manuscript received 1 March 2007; published 18 May 2007)

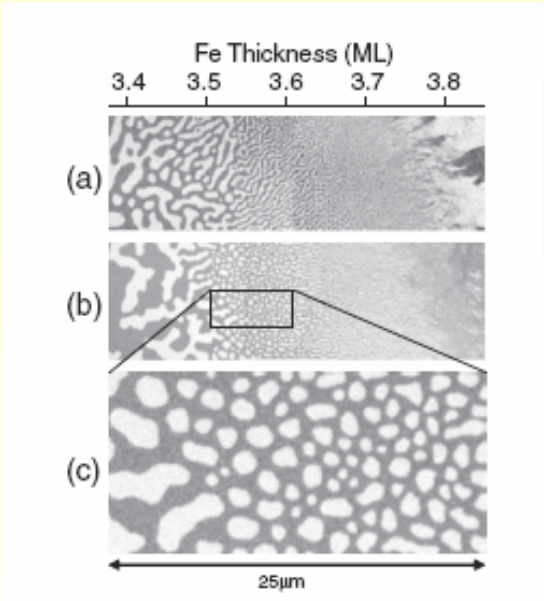

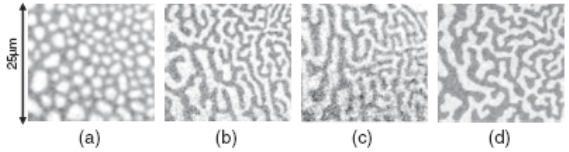

FIG. 4. Magnetic domain images of Fe(3.3 ML)/Ni(9 ML)/Cu(001) after applying a magnetic field pulse (a) less than ~5° from the sample surface, (b) ~10° from the sample surface, (c) ~20° from the sample surface, and (d) perpendicular to the sample surface.

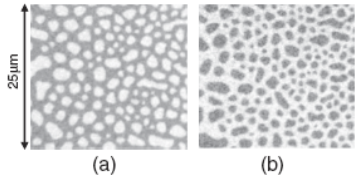

FIG. 3. Bubble domain phase of Fe(3.55 ML)/Ni(10.6 ML)/Cu(001) (a) after applying a nearly in-plane magnetic field pulse and (b) after applying a magnetic field pulse in the opposite direction. The reversal of the domain contrast shows that there exists a small normal component of the magnetic field pulse.

CONCLUSIONES

Que sabemos?

• Diagrama de fases a campo magnético cero:

$\delta = 3$

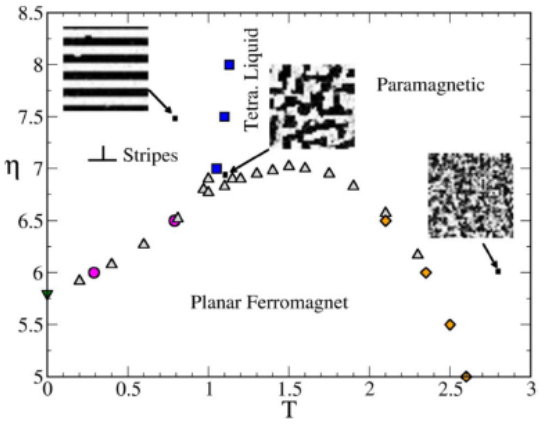

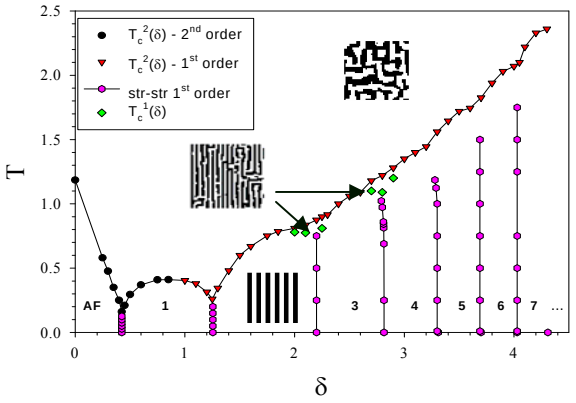

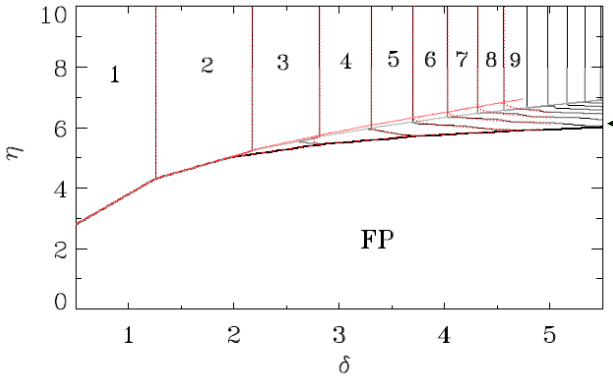

$T = 0$

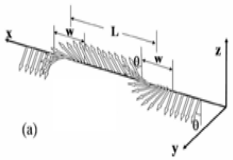

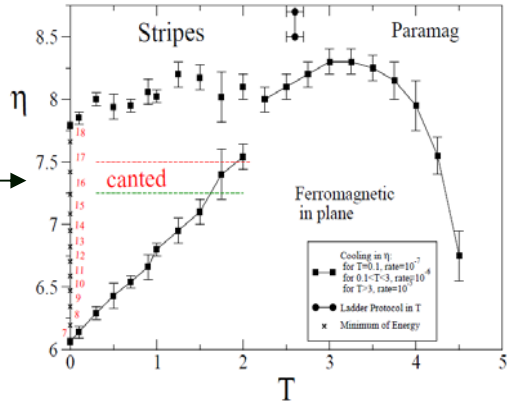

$\delta = 6$

• Rol de las anisotropías y las fluctuaciones

Que falta?

- Orden de las transiciones de fase
- Efectos de campos magnéticos externos
- Variación del ancho de fajas con la temperatura y el espesor de la lámina

1. Rol de la dinámica de defectos
2. Componentes de magnetización en el plano
3. Estructura de las paredes de dominio